Препринти Інституту фізики конденсованих систем НАН України розповсюджуються серед наукових та інформаційних установ. Вони також доступні по електронній комп'ютерній мережі на WWW-сервері інституту за адресою http://www.icmp.lviv.ua/

The preprints of the Institute for Condensed Matter Physics of the National Academy of Sciences of Ukraine are distributed to scientific and informational institutions. They also are available by computer network from Institute's WWW server (http://www.icmp.lviv.ua/)

Олег Олегович Менчишин
Тарас Євстахійович Крохмальський
Олег Володимирович Держко

Спін-1/2 модель Гайзенберга на простій кубічній гратці у методі функцій Гріна

Роботу отримано 10 червня 2014 р.

Затверджено до друку Вченою радою ІФКС НАН України

Рекомендовано до друку відділом теорії модельних спінових систем

Виготовлено при ІФКС НАН України

Національна академія наук України

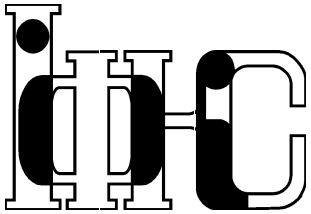

ІНСТИТУТ ФІЗИКИ КОНДЕНСОВАНИХ СИСТЕМ

ICMP–14–01E

Oleg Menchyshyn, Taras Krokhmalskii, Oleg Derzhko

SIMPLE-CUBIC-LATTICE SPIN-1/2 HEISENBERG MODEL WITHIN GREEN-FUNCTION METHOD

ЛЬВІВ

УДК: 537.9; 537.622

PACS: 75.10.Jm

Спін-1/2 модель Гайзенберга на простій кубічній гратці у методі функцій Гріна

Олег Менчишин, Тарас Крохмальський, Олег Держко

Анотація. Ми розглядаємо спін-1/2 модель Гайзенберга на простій кубічній гратці з феромагнітною чи антиферомагнітною взаємодією найближчих сусідів методом спін-ротаційно-інваріантних функцій Гріна другого порядку. Ми зосереджуємося на високотемпературній поведінці статичної сприйнятливості, яка може бути використана для визначення критичної температури моделі. Ми порівнюємо результати методу функцій Гріна з даними симуляцій методом квантового Монте Карло. Ми обговорюємо перспективи застосування методу функцій Гріна для вивчення високотемпературних властивостей фрустрованих квантових спінових систем.

Simple-cubic-lattice spin-1/2 Heisenberg model within Green-function method

Oleg Menchyshyn, Taras Krokhmalskii, Oleg Derzhko

Abstract. We consider the spin-1/2 Heisenberg model on a simple cubic lattice with ferromagnetic or antiferromagnetic nearest-neighbor interaction within the spin-rotation-invariant second-order Green-function method. We focus on the high-temperature behavior of the static susceptibility which can be used to determine the critical temperature of the model. We compare the Green-function results with the quantum Monte Carlo simulation data. We discuss perspectives for application of the Green-function method for the study of the high-temperature properties of frustrated quantum spin models.

1. Introduction

Competing interactions are known to have a drastic influence on the ground-state/low-temperature properties of lattice spin systems [1]. On the other hand, they can influence the finite-temperature properties too, in particular, the critical temperature T_c which separates a low-temperature ordered phase ($T < T_c$) and the high-temperature disordered phase ($T > T_c$). There are only a few methods which can be used to examine this issue. One among them is a two-time Green-function method. The two-time Green-function method is well known in the quantum spin system theory for more than fifty years due to seminal studies by N. N. Bogolyubov, S. V. Tyablikov, D. N. Zubarev and other researches [2–7]. Many further developments of the method as well as various specific applications have been reported until now. One special version of the Green-function approach which is applicable to quantum spin systems with frustration was suggested by Kondo and Yamaji [8]. Two-time Green functions can be found from the equation of motion after introducing some decoupling scheme [2–4, 7]. The Tyablikov decoupling [3] is used at the first stage but it is not a good one if the model does not have a long-range order. The Kondo-Yamaji decoupling [8] is used at the second stage of the equation of motion and it certainly improves the description. This so-called spin-rotation-invariant second-order Green-function method introduced in 1972 [8] was further developed and applied to Heisenberg magnets by several groups, see Refs. [9–13] and references therein.[1]

We intend to discuss the effect of frustration on the critical temperature of quantum Heisenberg magnets using the spin-rotation-invariant second-order Green-function method and begin with a test example. Namely, in the present study we exploit the Green-function method for studying the high-temperature properties and determining the critical temperature of the spin-1/2 Heisenberg magnet on a simple cubic lattice with ferro- or antiferromagnetic nearest-neighbor interaction. The idea of our calculations is as follows. We consider thermodynamic quantities in the region without long-range order, i.e., $T > T_c$, and calculate the Green function $\langle\langle s^+_{\mathbf{q}}; s^-_{\mathbf{q}}\rangle\rangle_\omega$. In the case of the ferromagnet, we define

[1] Here we need to comment shortly on the terminology we use. Namely, "second-order Green-function method" simply means that decoupling procedure is made on the second round of the equations of motion for the Green functions. "Proper" second-order theory for Green functions would mean a correct renormalization of the mass operator, leading to magnon decay. There was also a modification of the famous Callen decoupling from Yu. A. Tserkovnikov in [14] which keeps a spin-rotation invariance in the high-temperature region.

Table 1. The Curie temperature $T_{\rm C}$ of the simple-cubic-lattice spin-1/2 Heisenberg ferromagnet (in units of $|J|/k_{\rm B}$, $k_{\rm B}=1$) obtained within different methods.

QMC [18]	Tyablikov [3]	Kondo-Yamaji [12]	Kondo-Yamaji (present paper)
0.839(1)	0.989	0.926	0.926
100%	118%	110%	110%

the critical temperature for the ferromagnetic ordering $T_c = T_{\rm C}$ (the Curie temperature) as the temperature of the divergence of the uniform static susceptibility $\chi^{+-}_{\mathbf{q}=0,\omega=0}$. In the case of the antiferromagnet, we look for the temperature $T_c = T_{\rm N}$ (the Néel temperature) of the divergence of the staggered static susceptibility $\chi^{+-}_{\mathbf{q}=(\pi,\pi,\pi),\omega=0}$. Since the model is unfrustrated we can compare our findings with quantum Monte Carlo simulations [15–18] which we perform for completeness using the ALPS package [19].

The paper is organized as follows. In Sec. 2 we introduce the model and notations. In Sec. 3 we briefly illustrate the Tyablikov approximation, whereas in Sec. 4 and Appendices A and B we explain in some detail how to obtain the high-temperature thermodynamics within the Kondo-Yamaji approximation. In Sec. 4 we also compare our findings with the results of various authors as well as with the high-temperature expansions and the quantum Monte Carlo data. We make a summary and sketch perspectives for further studies in Sec. 5. Our conclusions concerning the critical temperatures are conveniently summarized in Tables 1 and 2.

2. The model. Green-function method

In this section, we introduce the model under consideration and notations for the Green-function technique. The Hamiltonian of the spin-1/2 isotropic Heisenberg model on a simple cubic lattice reads

$$H = J\sum_{\text{n.n.}} \mathbf{s}_i \cdot \mathbf{s}_j$$

Table 2. The Néel temperature $T_{\rm N}$ of the simple-cubic-lattice spin-1/2 Heisenberg antiferromagnet (in units of $J/k_{\rm B}$, $k_{\rm B}=1$) obtained within different methods.

QMC [18]	Tyablikov [3]	Kondo-Yamaji [12]	Kondo-Yamaji (present paper)
0.946(1)	$T_{\rm N}=T_{\rm C}$	1.079	1.041
100%	105%	114%	110%

$$= J\sum_{m_x=1}^{N_x}\sum_{m_y=1}^{N_y}\sum_{m_z=1}^{N_z}\left(\mathbf{s}_{\mathbf{m}}\cdot\mathbf{s}_{m_x+1}+\mathbf{s}_{\mathbf{m}}\cdot\mathbf{s}_{m_y+1}+\mathbf{s}_{\mathbf{m}}\cdot\mathbf{s}_{m_z+1}\right). \quad (2.1)$$

Here $J=-|J|<0$ corresponds to the ferromagnetic interaction and $J=|J|>0$ corresponds to the antiferromagnetic interaction, the first sum in Eq. (2.1) runs over all nearest-neighbor bonds on the simple cubic lattice of $N=N_xN_yN_z$ sites, and periodic boundary conditions are implied. In the second line of Eq. (2.1) we write down the sum over the nearest-neighbor bonds explicitly introducing convenient shorthand notations for further calculations. Furthermore, spin-1/2 operators satisfy the standard on-site commutation rules, $[s^+,s^-]_-=2s^z$, $[s^z,s^+]_-=s^+$, $[s^z,s^-]_-=-s^-$.

We introduce

$$s^{\pm}_{\mathbf{q}} = \frac{1}{\sqrt{N}}\sum_{\mathbf{m}} e^{\mp \mathrm{i}\mathbf{q}\cdot\mathbf{m}} s^{\pm}_{\mathbf{m}}, \quad (2.2)$$

where the sum runs over all N lattice sites. The (retarded) Green function is defined according to the following equations:

$$\langle\langle s^+_{\mathbf{q}}; s^-_{\mathbf{q}}\rangle\rangle_t \equiv \frac{1}{\mathrm{i}\hbar}\Theta(t)\langle[s^+_{\mathbf{q}}(t), s^-_{\mathbf{q}}(0)]_-\rangle,$$

$$\langle\langle s^+_{\mathbf{q}}; s^-_{\mathbf{q}}\rangle\rangle_\omega = \int_{-\infty}^{\infty} \mathrm{d}t e^{\mathrm{i}\omega t}\langle\langle s^+_{\mathbf{q}}; s^-_{\mathbf{q}}\rangle\rangle_t,$$

$$\langle\langle s^+_{\mathbf{q}}; s^-_{\mathbf{q}}\rangle\rangle_t = \frac{1}{2\pi}\int_{-\infty}^{\infty}\mathrm{d}\omega e^{-\mathrm{i}\omega t}\langle\langle s^+_{\mathbf{q}}; s^-_{\mathbf{q}}\rangle\rangle_{\omega+\mathrm{i}\epsilon}, \epsilon\to+0. \quad (2.3)$$

Here $\langle(\ldots)\rangle$ means the standard statistical mechanics average of $(\ldots)$, i.e., $\langle(\ldots)\rangle = \mathrm{Tr}(e^{-H/T}(\ldots))/\mathrm{Tr}(e^{-H/T})$.

Two-time Green functions can be found from the equation of motion after introducing some decoupling scheme [2–4, 7]. The equation of motion at the first stage reads:

$$\hbar\omega\langle\langle s^+_{\mathbf{q}}; s^-_{\mathbf{q}}\rangle\rangle_\omega = \frac{2}{N}\sum_{\mathbf{m}}\langle s^z_{\mathbf{m}}\rangle + \langle\langle \mathrm{i}\hbar\dot{s}^+_{\mathbf{q}}; s^-_{\mathbf{q}}\rangle\rangle_\omega \tag{2.4}$$

with $\langle s^z_{\mathbf{m}}\rangle = 0$ (rotational symmetry in spin space) in the disordered phase. The equation of motion for the Green function in the r.h.s. of Eq. (2.4) reads

$$\hbar\omega\langle\langle \mathrm{i}\hbar\dot{s}^+_{\mathbf{q}}; s^-_{\mathbf{q}}\rangle\rangle_\omega = \mathrm{i}\hbar\langle[\dot{s}^+_{\mathbf{q}}, s^-_{\mathbf{q}}]_-\rangle - \hbar^2\langle\langle \ddot{s}^+_{\mathbf{q}}; s^-_{\mathbf{q}}\rangle\rangle_\omega. \tag{2.5}$$

We will use in the Green function in the r.h.s. of Eq. (2.5) the Kondo-Yamaji decoupling [8]:

$$\begin{aligned} s^-_A s^+_B s^+_C &\to \eta_{AB}C_{AB}s^+_C + \eta_{AC}C_{AC}s^+_B, \\ s^z_A s^z_B s^+_C &\to \frac{1}{2}\eta_{AB}C_{AB}s^+_C, \end{aligned} \tag{2.6}$$

where we introduce the notation $C_{AB} = \langle s^-_A s^+_B\rangle$ and the relation $\langle s^-_A s^+_B\rangle = 2\langle s^z_A s^z_B\rangle$.

If the Green function $\langle\langle s^+_{\mathbf{q}}; s^-_{\mathbf{q}}\rangle\rangle_\omega$ is known, the correlation function $\langle s^-_{\mathbf{q}} s^+_{\mathbf{q}}\rangle$ follows from the relation:

$$\langle s^-_{\mathbf{q}} s^+_{\mathbf{q}}\rangle = \frac{\mathrm{i}\hbar}{2\pi}\lim_{\epsilon\to+0}\int_{-\infty}^{\infty}\mathrm{d}\omega\frac{\langle\langle s^+_{\mathbf{q}}; s^-_{\mathbf{q}}\rangle\rangle_{\omega+\mathrm{i}\epsilon} - \langle\langle s^+_{\mathbf{q}}; s^-_{\mathbf{q}}\rangle\rangle_{\omega-\mathrm{i}\epsilon}}{e^{\frac{\hbar\omega}{T}}-1}, \tag{2.7}$$

see Ref. [2]. Thus, Eq. (2.7) gives the correlation function $\langle s^-_{\mathbf{q}} s^+_{\mathbf{q}}\rangle$ and therefore the correlation functions

$$\langle s^-_{\mathbf{m}} s^+_{\mathbf{m}+\mathbf{a}}\rangle = \frac{1}{N}\sum_{\mathbf{q}} e^{\mathrm{i}\mathbf{q}\cdot\mathbf{a}}\langle s^-_{\mathbf{q}} s^+_{\mathbf{q}}\rangle, \tag{2.8}$$

i.e.,

$$\begin{aligned} C_{000} = \langle s^- s^+\rangle = \frac{1}{2} - \langle s^z\rangle &= \frac{1}{N}\sum_{\mathbf{q}}\langle s^-_{\mathbf{q}} s^+_{\mathbf{q}}\rangle, \\ C_{100} &= \frac{1}{N}\sum_{\mathbf{q}} e^{\mathrm{i}q_x}\langle s^-_{\mathbf{q}} s^+_{\mathbf{q}}\rangle, \\ C_{110} &= \frac{1}{N}\sum_{\mathbf{q}} e^{\mathrm{i}(q_x+q_y)}\langle s^-_{\mathbf{q}} s^+_{\mathbf{q}}\rangle, \\ C_{200} &= \frac{1}{N}\sum_{\mathbf{q}} e^{2\mathrm{i}q_x}\langle s^-_{\mathbf{q}} s^+_{\mathbf{q}}\rangle \end{aligned} \tag{2.9}$$

etc.. As a result, all thermodynamic quantities can be found. For example, the internal energy (per site) reads

$$e(T) = 3J\left(\langle s^x_{\mathbf{m}} s^x_{m_x+1}\rangle + \langle s^y_{\mathbf{m}} s^y_{m_x+1}\rangle + \langle s^z_{\mathbf{m}} s^z_{m_x+1}\rangle\right) = \frac{9}{2}JC_{100}. \tag{2.10}$$

On the other hand, the Green function $\langle\langle s^+_{\mathbf{q}}; s^-_{\mathbf{q}}\rangle\rangle_\omega$ is directly related to the (isolated) dynamic transverse spin susceptibility $\chi^{+-}_{\mathbf{q},\omega}$,

$$\chi^{+-}_{\mathbf{q},\omega} = -\langle\langle s^+_{\mathbf{q}}; s^-_{\mathbf{q}}\rangle\rangle_\omega, \tag{2.11}$$

see Ref. [2], bearing in such a way also nonequilibrium properties of the model at hand within a linear response theory.

3. Tyablikov decoupling: Approaching T_c from below

Consider at first the ferromagnetic case $J = -|J| < 0$. Within the Tyablikov approximation $s^z_A s^+_B \to \langle s^z_A\rangle s^+_B$ resulting in

$$\langle\langle s^+_{\mathbf{q}}; s^-_{\mathbf{q}}\rangle\rangle_\omega = \frac{2\langle s^z\rangle}{\hbar\omega - 6|J|\left(1-\gamma_{\mathbf{q}}\right)\langle s^z\rangle}, \tag{3.1}$$

where $\gamma_{\mathbf{q}} = \left(\cos q_x + \cos q_y + \cos q_z\right)/3$ and $\langle s^z\rangle = 1/2 - C_{000}$ satisfies the following equation:

$$\frac{1}{2} - \langle s^z\rangle = \frac{1}{N}\sum_{\mathbf{q}}\frac{2\langle s^z\rangle}{e^{6|J|(1-\gamma_{\mathbf{q}})\langle s^z\rangle/T}-1}. \tag{3.2}$$

$\langle s^z\rangle$ equals zero in the high-temperature phase and starts to deviate from zero at T_c which therefore satisfies the equation

$$\begin{aligned} \frac{3|J|}{2T_c} &= \frac{1}{N}\sum_{\mathbf{q}}\frac{1}{1-\gamma_{\mathbf{q}}} \\ &= \frac{1}{\pi^3}\int_0^\pi \mathrm{d}x\int_0^\pi \mathrm{d}y\int_0^\pi \mathrm{d}z\frac{3}{3-\cos x-\cos y-\cos z} \\ &\approx 1.516\,386, \end{aligned} \tag{3.3}$$

see Ref. [20]. From this equation we get for the Curie temperature $T_{\mathrm{C}} \approx 0.989|J|$, see Ref. [3]. In the high-temperature phase the Green function $\langle\langle s^+_{\mathbf{q}}; s^-_{\mathbf{q}}\rangle\rangle_\omega$ is zero that indicates that the Tyablikov approximation is too crude and violates ergodicity [4]. (However, it is still possible to get $\langle s^-_{\mathbf{q}} s^+_{\mathbf{q}}\rangle$, see Ref. [4].)

In the antiferromagnetic case $J = |J| > 0$, one may perform a π-rotation over y-axis in the spin space for one of two sublattices of the simple-cubic lattice arriving at the simple-cubic-lattice spin-1/2 Hamiltonian with the ferromagnetic but anisotropic interaction

$$H = -|J| \sum_{\text{n.n.}} \left(s_i^x s_j^x - s_i^y s_j^y + s_i^z s_j^z \right). \tag{3.4}$$

Introducing in addition to the Green function (2.3) the Green function $\langle\langle s^-_{-\mathbf{q}}; s^-_{\mathbf{q}} \rangle\rangle_t$, within the Tyablikov approximation we may find

$$\begin{aligned} \langle\langle s^+_{\mathbf{q}}; s^-_{\mathbf{q}} \rangle\rangle_\omega &= \frac{2\langle s^z \rangle \left(\hbar\omega + 6|J|\langle s^z \rangle \right)}{(\hbar\omega)^2 - 36|J|^2 \left(1 - \gamma_{\mathbf{q}}^2\right) \langle s^z \rangle^2} \\ &= \frac{\hbar\omega + 6|J|\langle s^z \rangle}{6|J|\sqrt{1-\gamma_{\mathbf{q}}^2}} \\ \times \left(\frac{1}{\hbar\omega - 6|J|\sqrt{1-\gamma_{\mathbf{q}}^2}\langle s^z \rangle} - \frac{1}{\hbar\omega + 6|J|\sqrt{1-\gamma_{\mathbf{q}}^2}\langle s^z \rangle} \right). \end{aligned} \tag{3.5}$$

As a result, we arrive at the following equation for $\langle s^z \rangle$

$$\begin{aligned} \frac{1}{2} - \langle s^z \rangle &= \frac{1}{N} \sum_{\mathbf{q}} \frac{\left(\sqrt{1-\gamma_{\mathbf{q}}^2} + 1 \right) \langle s^z \rangle}{\sqrt{1-\gamma_{\mathbf{q}}^2} \left(e^{6|J|\sqrt{1-\gamma_{\mathbf{q}}^2}\langle s^z \rangle / T} - 1 \right)} \\ &+ \frac{1}{N} \sum_{\mathbf{q}} \frac{\left(\sqrt{1-\gamma_{\mathbf{q}}^2} - 1 \right) \langle s^z \rangle}{\sqrt{1-\gamma_{\mathbf{q}}^2} \left(e^{-6|J|\sqrt{1-\gamma_{\mathbf{q}}^2}\langle s^z \rangle / T} - 1 \right)} \end{aligned} \tag{3.6}$$

and the following formula for the Néel temperature $T_{\text{N}} = T_c$:

$$\begin{aligned} \frac{3|J|}{2T_c} &= \frac{1}{N} \sum_{\mathbf{q}} \frac{1}{1-\gamma_{\mathbf{q}}^2} \\ &= \frac{1}{2N} \sum_{\mathbf{q}} \frac{1}{1-\gamma_{\mathbf{q}}} + \frac{1}{2N} \sum_{\mathbf{q}} \frac{1}{1+\gamma_{\mathbf{q}}} \\ &= \frac{1}{2\pi^3} \int_0^\pi \mathrm{d}x \int_0^\pi \mathrm{d}y \int_0^\pi \mathrm{d}z \frac{3}{3 - \cos x - \cos y - \cos z} \\ &+ \frac{1}{2\pi^3} \int_0^\pi \mathrm{d}x \int_0^\pi \mathrm{d}y \int_0^\pi \mathrm{d}z \frac{3}{3 + \cos x + \cos y + \cos z} \\ &\approx 1.516\,386 \end{aligned} \tag{3.7}$$

since the second integral transforms into the first one after the change of the variables $x' = \pi - x$, $y' = \pi - y$, $z' = \pi - z$. Thus, $T_{\text{N}} = T_{\text{C}}$ [3]. For further details concerning the Tyablikov approximation see Refs. [3, 4] and references therein.

In summary, the high-temperature quantities within the Tyablikov approximation are hard to calculate straightforwardly and therefore this decoupling in the equation of motion for $\langle\langle s^+_{\mathbf{q}}; s^-_{\mathbf{q}} \rangle\rangle_\omega$ is hard to use for pinning down the critical temperature T_c coming from the high-temperature limit. Besides the fact that the Tyablikov approximation is not straightforward in the high-temperature phase, after all, the Kondo-Yamaji decoupling is the next step after the Tyablikov decoupling. Therefore the Kondo-Yamaji decoupling is expected to provide a better description. However, the Tyablikov approximation may be used while studying T_c approaching it from below.

4. Kondo-Yamaji decoupling in the disordered phase

4.1. Analytical results

Within the Kondo-Yamaji approximation (2.6) we have the following result for the Green function:

$$\begin{aligned} \langle\langle s^+_{\mathbf{q}}; s^-_{\mathbf{q}} \rangle\rangle_\omega &= \frac{M_{\mathbf{q}}}{(\hbar\omega)^2 - (\hbar\omega_{\mathbf{q}})^2} \\ &= \frac{M_{\mathbf{q}}}{2\hbar\omega_{\mathbf{q}}} \left(\frac{1}{\hbar\omega - \hbar\omega_{\mathbf{q}}} - \frac{1}{\hbar\omega + \hbar\omega_{\mathbf{q}}} \right), \\ M_{\mathbf{q}} &= -12JC_{100}\left(1 - \gamma_{\mathbf{q}}\right), \\ \left(\frac{\hbar\omega_{\mathbf{q}}}{J} \right)^2 &= 3\left(1 - \gamma_{\mathbf{q}}\right)\left(1 + 10\eta_{100}C_{100}\right. \\ &\left. + 8\eta_{110}C_{110} + 2\eta_{200}C_{200} - 12\eta_{100}C_{100}\left(1 + \gamma_{\mathbf{q}}\right)\right), \end{aligned} \tag{4.1}$$

where $\gamma_{\mathbf{q}} = \left(\cos q_x + \cos q_y + \cos q_z\right)/3$, see Appendix A for details of calculations.

The obtained result contains three unknown correlation functions C_{100}, C_{110}, C_{200} and the corresponding parameters η_{100}, η_{110}, η_{200}. We assume that $\eta_{100} = \eta_{110} = \eta_{200} = \eta$ [these parameters (for the antiferromagnetic case at low temperatures) can be determined using some additional conditions beyond the standard prescriptions, see, e.g., Refs. [12, 13] and references therein]. From Eq. (4.1) we find the imaginary part of the Green function

$$\langle\langle s^+_{\mathbf{q}}; s^-_{\mathbf{q}} \rangle\rangle_{\omega + \mathrm{i}\epsilon} - \langle\langle s^+_{\mathbf{q}}; s^-_{\mathbf{q}} \rangle\rangle_{\omega - \mathrm{i}\epsilon}$$

$$= -2\pi \mathrm{i} \frac{M_{\mathbf{q}}}{2\hbar\omega_{\mathbf{q}}} \left(\delta(\hbar\omega - \hbar\omega_{\mathbf{q}}) - \delta(\hbar\omega + \hbar\omega_{\mathbf{q}})\right) \tag{4.2}$$

and evaluate the r.h.s. in Eq. (2.7)

$$\frac{\mathrm{i}\hbar}{2\pi} \lim_{\epsilon\to+0} \int_{-\infty}^{\infty} \mathrm{d}\omega \frac{\langle\langle s^+_{\mathbf{q}}; s^-_{\mathbf{q}}\rangle\rangle_{\omega+\mathrm{i}\epsilon} - \langle\langle s^+_{\mathbf{q}}; s^-_{\mathbf{q}}\rangle\rangle_{\omega-\mathrm{i}\epsilon}}{e^{\frac{\hbar\omega}{T}} - 1}$$
$$= \frac{M_{\mathbf{q}}}{2\hbar\omega_{\mathbf{q}}} \left(\frac{1}{e^{\frac{\hbar\omega_{\mathbf{q}}}{T}} - 1} - \frac{1}{e^{-\frac{\hbar\omega_{\mathbf{q}}}{T}} - 1} \right)$$
$$= \frac{M_{\mathbf{q}}}{2\hbar\omega_{\mathbf{q}}} \left(1 + \frac{2}{e^{\frac{\hbar\omega_{\mathbf{q}}}{T}} - 1} \right). \tag{4.3}$$

Thus, we have obtained the correlation function

$$\langle s^-_{\mathbf{q}} s^+_{\mathbf{q}}\rangle = \frac{M_{\mathbf{q}}}{2\hbar\omega_{\mathbf{q}}} \left(1 + \frac{2}{e^{\frac{\hbar\omega_{\mathbf{q}}}{T}} - 1} \right) \tag{4.4}$$

which, according to Eq. (2.2), is related to the site-site correlation functions

$$\langle s^-_{\mathbf{q}} s^+_{\mathbf{q}}\rangle = \frac{1}{N} \sum_{\mathbf{m}_1} \sum_{\mathbf{m}_2} e^{\mathrm{i}\mathbf{q}\cdot(\mathbf{m}_1 - \mathbf{m}_2)} \langle s^-_{\mathbf{m}_1} s^+_{\mathbf{m}_2}\rangle = \sum_{\mathbf{a}} e^{-\mathrm{i}\mathbf{q}\cdot\mathbf{a}} \langle s^-_{\mathbf{m}} s^+_{\mathbf{m}+\mathbf{a}}\rangle. \tag{4.5}$$

Inverting the latter formula we get

$$\langle s^-_{\mathbf{m}} s^+_{\mathbf{m}+\mathbf{a}}\rangle = \frac{1}{N} \sum_{\mathbf{q}} e^{\mathrm{i}\mathbf{q}\cdot\mathbf{a}} \langle s^-_{\mathbf{q}} s^+_{\mathbf{q}}\rangle \tag{4.6}$$

[cf. Eq. (2.8)] and in particular

$$C_{000} = \langle s^- s^+\rangle = \frac{1}{2} - \langle s^z\rangle = \frac{1}{2}, \quad C_{000} = \frac{1}{N} \sum_{\mathbf{q}} \langle s^-_{\mathbf{q}} s^+_{\mathbf{q}}\rangle,$$
$$C_{100} = \frac{1}{N} \sum_{\mathbf{q}} e^{\mathrm{i}q_x} \langle s^-_{\mathbf{q}} s^+_{\mathbf{q}}\rangle,$$
$$C_{110} = \frac{1}{N} \sum_{\mathbf{q}} e^{\mathrm{i}(q_x+q_y)} \langle s^-_{\mathbf{q}} s^+_{\mathbf{q}}\rangle,$$
$$C_{200} = \frac{1}{N} \sum_{\mathbf{q}} e^{2\mathrm{i}q_x} \langle s^-_{\mathbf{q}} s^+_{\mathbf{q}}\rangle \tag{4.7}$$

[cf. Eq. (2.9)], where in the thermodynamic limit the sum should be replaced by the three-fold integral

$$\frac{1}{N} \sum_{\mathbf{q}} (\ldots) \to \frac{1}{(2\pi)^3} \int_{-\pi}^{\pi} \mathrm{d}q_x \int_{-\pi}^{\pi} \mathrm{d}q_y \int_{-\pi}^{\pi} \mathrm{d}q_z (\ldots). \tag{4.8}$$

These equations for η, C_{100}, C_{110}, C_{200} [i.e., Eqs. (4.7), (4.8), (4.4), (4.1)] will be solved numerically starting from the high-temperature limit.

Let us discuss how to determine the critical temperature T_c. Consider the ferromagnetic case $J = -|J| < 0$. To find T_c, we may examine the behavior of the uniform static susceptibility $\chi^{+-}_{\mathbf{q}=0,\omega=0}$ as temperature decreases starting from infinite value. If $\chi^{+-}_{\mathbf{q}=0,\omega=0} \to \infty$ that would mean that $T \to T_c = T_{\mathrm{C}}$. From Eq. (4.1) we have

$$\chi^{+-}_{\mathbf{q}=0,\omega=0} = -\frac{\frac{4C_{100}}{J}}{1 - 14\eta C_{100} + 8\eta C_{110} + 2\eta C_{200}} \tag{4.9}$$

and $\chi^{+-}_{\mathbf{q}=0,\omega=0}$ diverges when

$$1 - 14\eta C_{100} + 8\eta C_{110} + 2\eta C_{200} \to 0. \tag{4.10}$$

For the antiferromagnetic case $J = |J| > 0$, we have to examine the staggered static susceptibility

$$\chi^{+-}_{\mathbf{q}=(\pi,\pi,\pi),\omega=0} = -\frac{\frac{4C_{100}}{J}}{1 + 10\eta C_{100} + 8\eta C_{110} + 2\eta C_{200}} \tag{4.11}$$

which diverges when

$$1 + 10\eta C_{100} + 8\eta C_{110} + 2\eta C_{200} \to 0 \tag{4.12}$$

in this way giving the critical temperature $T_c = T_{\mathrm{N}}$.

The magnetic correlation length ξ above T_c may be calculated by expanding $\chi^{+-}_{\mathbf{q}=(0+k_x,0+k_y,0+k_z),\omega=0}$ in the neighborhood of the vector $\mathbf{q} = (0,0,0)$ or $\chi^{+-}_{\mathbf{q}=(\pi+k_x,\pi+k_y,\pi+k_z),\omega=0}$ in the neighborhood of the vector $\mathbf{q} = (\pi,\pi,\pi)$. For the ferromagnet the expansion yields

$$\chi^{+-}_{\mathbf{q}=(0+k_x,0+k_y,0+k_z),\omega=0} = \frac{\chi^{+-}_{\mathbf{q}=(0,0,0),\omega=0}}{1 + \xi^2 k^2},$$
$$\xi^2 = \frac{2\eta C_{100}}{1 - 14\eta C_{100} + 8\eta C_{110} + 2\eta C_{200}}. \tag{4.13}$$

For the antiferromagnet the expansion yields

$$\chi^{+-}_{\mathbf{q}=(\pi+k_x,\pi+k_y,\pi+k_z),\omega=0} = \frac{\chi^{+-}_{\mathbf{q}=(\pi,\pi,\pi),\omega=0}}{1+\xi^2 k^2},$$
$$\xi^2 = \frac{-2\eta C_{100}}{1+10\eta C_{100}+8\eta C_{110}+2\eta C_{200}}. \qquad (4.14)$$

We may also examine the temperature dependence of the specific heat (per site)

$$c(T) = \frac{\partial}{\partial T}\left(3J\frac{3}{2}C_{100}\right) = \frac{9}{2}J\frac{\partial C_{100}}{\partial T}, \qquad (4.15)$$

which should signalize the approach to T_c from above.

4.2. Numerical results. Critical temperature

To solve the equations for η, C_{100}, C_{110}, C_{200}, we begin with analytical results in the high-temperature limit, see Appendix B. It can be shown that the first nonvanishing terms for the unknown quantities η, C_{100}, C_{110}, C_{200} in the series with respect to J/T behave as follows:

$$\eta = 1 + o(1),$$
$$C_{100} = -\frac{1}{8}\frac{J}{T} + o\left(\frac{J}{T}\right) = C^{\mathrm{HT}}_{100} + o\left(\frac{J}{T}\right),$$
$$C_{110} = \frac{1}{16}\left(\frac{J}{T}\right)^2 + o\left(\left(\frac{J}{T}\right)^2\right) = C^{\mathrm{HT}}_{110} + o\left(\left(\frac{J}{T}\right)^2\right),$$
$$C_{200} = \frac{1}{32}\left(\frac{J}{T}\right)^2 + o\left(\left(\frac{J}{T}\right)^2\right) = C^{\mathrm{HT}}_{200} + o\left(\left(\frac{J}{T}\right)^2\right). \qquad (4.16)$$

We use these formulas in a numerical solution described below. More specific, first of all we introduce the notations $\tilde{C}_{\alpha\beta\gamma} = \eta C_{\alpha\beta\gamma}$ and notice that the latter three equations in Eq. (4.7) do not contain η, i.e., they are equations for $\tilde{C}_{\alpha\beta\gamma}$, whereas η follows from the first equation in Eq. (4.7) after $\tilde{C}_{\alpha\beta\gamma}$ are found. Furthermore, using the high-temperature results $\tilde{C}^{\mathrm{HT}}_{\alpha\beta\gamma}(T)$ (4.16) we obtain the initial point $\tilde{C}^{*}_{\alpha\beta\gamma}(T=5) = \tilde{C}^{\mathrm{HT}}_{\alpha\beta\gamma}(T=5)$. Then we consider a cube $[\tilde{C}^{*}_{\alpha\beta\gamma} - \tilde{C}^{*}_{\alpha\beta\gamma}/2 \ldots \tilde{C}^{*}_{\alpha\beta\gamma} + \tilde{C}^{*}_{\alpha\beta\gamma}/2]$ and calculate the value of the objective (goal) function $\mathcal{F} = (\tilde{C}_{100} - \eta(1/N)\sum_{\mathbf{q}} e^{\mathrm{i}q_x}\langle s^-_{\mathbf{q}} s^+_{\mathbf{q}}\rangle)^2 + (\tilde{C}_{110} - \eta(1/N)\sum_{\mathbf{q}} e^{\mathrm{i}(q_x+q_y)}\langle s^-_{\mathbf{q}} s^+_{\mathbf{q}}\rangle)^2 + (\tilde{C}_{200} - \eta(1/N)\sum_{\mathbf{q}} e^{2\mathrm{i}q_x}\langle s^-_{\mathbf{q}} s^+_{\mathbf{q}}\rangle)^2$ which

follows from Eqs. (4.7) within this cube with the step $(\Delta\tilde{C}_{\alpha\beta\gamma})^{(1)} = \tilde{C}^{*}_{\alpha\beta\gamma}/m$, $m = 50$ or 100. We determine the values of $\tilde{C}^{(1)}_{\alpha\beta\gamma}$ for which the objective function attains its minimum. Then we consider a cube $[\tilde{C}^{(1)}_{\alpha\beta\gamma} - 2(\Delta\tilde{C}_{\alpha\beta\gamma})^{(1)} \ldots \tilde{C}^{(1)}_{\alpha\beta\gamma} + 2(\Delta\tilde{C}_{\alpha\beta\gamma})^{(1)}]$ and calculate the value of the objective function $\mathcal{F}$ with the step $(\Delta\tilde{C}_{\alpha\beta\gamma})^{(2)} = 4(\Delta\tilde{C}_{\alpha\beta\gamma})^{(1)}/m$, obtaining as a result the values of $\tilde{C}^{(2)}_{\alpha\beta\gamma}$ for which the objective function attains its minimum. We repeat this procedure k times ($k = \{10, 12, 15\}$). As a result, we obtain the solutions of Eqs. (4.7) at $T = 5$, say, $\tilde{C}_{\alpha\beta\gamma}(T=5) = \tilde{C}^{(15)}_{\alpha\beta\gamma}(T=5)$. Similarly, we obtain the solutions of Eqs. (4.7) at $T = 5 + 0.1$, $\tilde{C}_{\alpha\beta\gamma}(T = 5+0.1)$. Using these two points for linear extrapolation we obtain the initial point $\tilde{C}^{*}_{\alpha\beta\gamma}(T = 5-0.1)$. [Note that we do not use the high-temperature results to obtain the initial point $\tilde{C}^{*}_{\alpha\beta\gamma}(T=5-0.1)$. In fact, it is indeed impossible to use the high-temperature results for getting the initial point at, say, $T = 2$.] We repeat the procedure of seeking for the minimum of the objective function $\mathcal{F}$ starting from the cube $[\tilde{C}^{*}_{\alpha\beta\gamma} - 2\Delta\tilde{C}_{\alpha\beta\gamma} \ldots \tilde{C}^{*}_{\alpha\beta\gamma} + 2\Delta\tilde{C}_{\alpha\beta\gamma}]$, where $\Delta\tilde{C}_{\alpha\beta\gamma} \equiv \tilde{C}^{*}_{\alpha\beta\gamma}(T=5-0.1) - \tilde{C}_{\alpha\beta\gamma}(T=5)$. Proceeding in such a way with gradual decrease of the temperature T, we find all solutions of Eqs. (4.7). Moreover, after reaching $T = 2$ we decrease the temperature step from 0.1 to 0.02 (and to 0.01 for lower temperatures).

For the ferromagnetic case $J = -|J| < 0$, we report the obtained results for η, C_{100}, C_{110}, C_{200} along with the susceptibility (4.9) and the denominator in Eq. (4.9) which is given in the l.h.s. of Eq. (4.10) in Fig. 1. The denominator vanishes at $T_c = T_{\mathrm{C}} \approx 0.926|J|$.

For the antiferromagnetic case $J = |J| > 0$, the obtained results for η, C_{100}, C_{110}, C_{200} along with the susceptibility (4.11) and the denominator in Eq. (4.11) which is given in the l.h.s. of Eq. (4.12) are reported in Fig. 2. The denominator vanishes at $T_c = T_{\mathrm{N}} \approx 1.041J$.

Knowing the correlation functions, one can find, e.g., the magnetic correlation length $\xi(T)$, see Eqs. (4.13), (4.14), or the specific heat $c(T)$, see Eq. (4.15). The results for the specific heat are shown in the corresponding panels in Figs. 3 and 4 and in Fig. 5.

4.3. Comparison with another Green-function papers

Similar problems were studied within the Green-function method in the past [12, 21–28].

In particular, A. F. Barabanov with coauthors [25] obtained the fol-

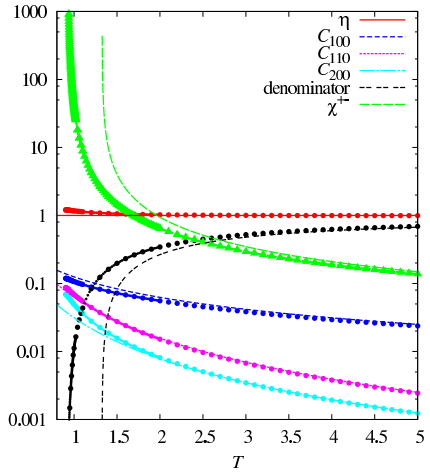

Figure 1. (Color online) Temperature dependence ($T = 0.8 \ldots 5$) of correlation functions C_{100}, C_{110}, C_{200}, and η for the case $J = -|J| < 0$ ($|J| = 1$) obtained numerically (circles). Curves correspond to the high-temperature asymptotics given in Eq. (4.16) (solid, short-dashed, dotted, and dash-dotted curves correspond to η, C_{100}, C_{110}, and C_{200}, respectively). In the high-temperature limit the asymptotics and the numerical solutions coincide. We also show the susceptibility $\chi^{+-}_{\mathbf{q}=0,\omega=0}$ (4.9) [long-dashed green curve with (without) up-triangles correspond to the numerical solution (high-temperature asymptotic)] and the l.h.s. of Eq. (4.10) [dash-dashed black curve with (without) circles correspond to the numerical solution (high-temperature asymptotic)]. The denominator in Eq. (4.9) vanishes at $T_c \approx 0.926$.

lowing expression for Green's function and spin excitation spectrum:

$$G^{\sigma}(\mathbf{q},\omega) = \frac{-12JK_{\mathbf{g}}\,(1-\gamma_{\mathbf{q}})}{\omega^2-\omega_{\mathbf{q}}^2},$$

$$\begin{aligned}\left(\frac{\omega_{\mathbf{q}}}{J}\right)^2 &= 6\,(1-\gamma_{\mathbf{q}})\left(6\alpha K_{\mathbf{g}}+\frac{1}{2}-\alpha K_{\mathbf{g}}\,(1+6\gamma_{\mathbf{q}})\right)\\ &= 3\,(1-\gamma_{\mathbf{q}})\,(1+12\alpha K_{\mathbf{g}}-\alpha K_{\mathbf{g}}\,(2+12\gamma_{\mathbf{q}}))\\ &= 3\,(1-\gamma_{\mathbf{q}})\,(1+22\alpha K_{\mathbf{g}}-12\alpha K_{\mathbf{g}}\,(1+\gamma_{\mathbf{q}}))\end{aligned} \qquad (4.17)$$

[see Eqs. (5) and (6) of this paper in the case $J_2 = 0$]. This result

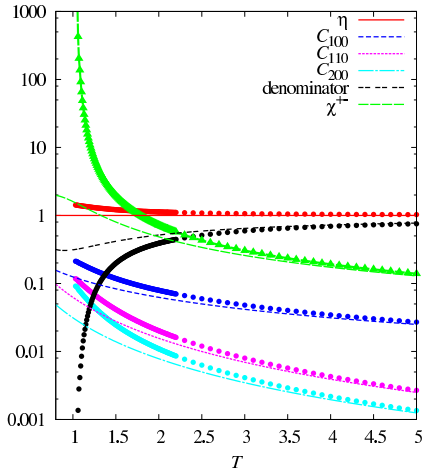

Figure 2. (Color online) Temperature dependence ($T = 0.8 \ldots 5$) of correlation functions C_{100}, C_{110}, C_{200}, and η for the case $J = |J| > 0$ ($|J| = 1$) obtained numerically (circles). Curves correspond to the high-temperature asymptotics given in Eq. (4.16) (solid, short-dashed, dotted, and dash-dotted curves correspond to η, C_{100}, C_{110}, and C_{200}, respectively). In the high-temperature limit the asymptotics and the numerical solutions coincide. We also show the susceptibility $\chi^{+-}_{\mathbf{q}=(\pi,\pi,\pi),\omega=0}$ (4.11) [long-dashed green curve with (without) up-triangles correspond to the numerical solution (high-temperature asymptotic)] and the l.h.s. of Eq. (4.12) [dash-dashed black curve with (without) circles correspond to the numerical solution (high-temperature asymptotic)]. The denominator in Eq. (4.11) vanishes at $T_c \approx 1.041$.

correspond to our findings given in Eq. (4.1) if

$$10\eta C_{100} + 8\eta C_{110} + 2\eta C_{200} \to 22\alpha K_{\mathbf{g}}. \qquad (4.18)$$

Note, that the result of A. F. Barabanov with coauthors [25] does not contain C_{110} and C_{200}.

Later on, in Ref. [12] the thermodynamics of layered Heisenberg magnets with arbitrary spin was investigated within the second-order Green-function technique. The authors consider an arbitrary spin value $s \geq 1/2$ and two different bonds, the in-plane bonds $J_{\|}$ and the inter-plane bonds $J_{\perp}$. In their study, they introduce several different vertex parameters η (denoted $\alpha_{1\mu}$, $\alpha_{2\mu}$ with $\mu = \|, \perp$) and find for $s = 1/2$ and

$J_\perp/J_\parallel = 1$ the Curie temperature $T_\mathrm{C} \approx 0.926|J_\parallel|$ and the Néel temperature $T_\mathrm{N} \approx 1.079 J_\parallel$, see Table II of Ref. [12]. The obtained in Ref. [12] Green function is given in Eqs. (5), (2), (6) – (9) of this paper. For the case $s = 1/2$, when the vertex parameter $\lambda_\mu = 0$, it can be written as

$$\langle\langle s^+_{\mathbf{q}}; s^-_{-\mathbf{q}}\rangle\rangle_\omega = \frac{M_{\mathbf{q}}}{\omega^2 - \omega^2_{\mathbf{q}}},$$

$$\begin{aligned}
M_{\mathbf{q}} &= -8J_\parallel C_{100}\left(1 - \frac{\cos q_x + \cos q_y}{2}\right) - 4J_\perp C_{001}\left(1 - \cos q_z\right), \\
\omega^2_{\mathbf{q}} &= \left(1 - \frac{\cos q_x + \cos q_y}{2}\right) \\
&\times \left(\Delta_\parallel + 16J^2_\parallel \alpha_{1\parallel} C_{100}\left(1 - \frac{\cos q_x + \cos q_y}{2}\right)\right) \\
&+ \left(1 - \cos q_z\right)\left(\Delta_\perp + 4J^2_\perp \alpha_{1\perp} C_{001}\left(1 - \cos q_z\right)\right) \\
&+ \tilde{\Delta}\left(1 - \frac{\cos q_x + \cos q_y}{2}\right)\left(1 - \cos q_z\right) \quad (4.19)
\end{aligned}$$

with

$$\begin{aligned}
\Delta_\parallel &= 2J^2_\parallel\left(1 + 2\alpha_{2\parallel}\left(2C_{110} + C_{200}\right) - 10\alpha_{1\parallel}C_{100}\right) \\
&+ 8J_\parallel J_\perp\left(\alpha_{2\perp}C_{101} - \alpha_{1\parallel}C_{100}\right), \\
\Delta_\perp &= J^2_\perp\left(1 + 2\alpha_{2\perp}C_{002} - 6\alpha_{1\perp}C_{001}\right) \\
&+ 8J_\parallel J_\perp\left(\alpha_{2\perp}C_{101} - \alpha_{1\perp}C_{001}\right), \\
\tilde{\Delta} &= 8J_\parallel J_\perp\left(\alpha_{1\parallel}C_{100} + \alpha_{1\perp}C_{001}\right). \quad (4.20)
\end{aligned}$$

For the case $J_\parallel = J_\perp = J$ we have to put $C_{001} = C_{100}$, $C_{101} = C_{110}$, $C_{002} = C_{200}$ and $\alpha_{1\parallel} = \alpha_{1\perp} = \alpha_1$, $\alpha_{2\parallel} = \alpha_{2\perp} = \alpha_2$. Therefore instead of Eq. (4.20) we have

$$\begin{aligned}
\Delta_\parallel &= 2J^2\left(1 - 14\alpha_1 C_{100} + 8\alpha_2 C_{110} + 2\alpha_2 C_{200}\right), \\
\Delta_\perp &= J^2\left(1 - 14\alpha_1 C_{100} + 8\alpha_2 C_{110} + 2\alpha_2 C_{200}\right), \\
\tilde{\Delta} &= 16J^2\alpha_1 C_{100}. \quad (4.21)
\end{aligned}$$

As a result,

$$\begin{aligned}
\left(\frac{\omega_{\mathbf{q}}}{J}\right)^2 &= \left(1 - \frac{\cos q_x + \cos q_y}{2}\right) \\
&\times \left(2\left(1 - 14\alpha_1 C_{100} + 8\alpha_2 C_{110} + 2\alpha_2 C_{200}\right)\right. \\
&\left. + 16\alpha_1 C_{100}\left(1 - \frac{\cos q_x + \cos q_y}{2}\right)\right) \\
&+ \left(1 - \cos q_z\right) \\
&\times \left(1 - 14\alpha_1 C_{100} + 8\alpha_2 C_{110} + 2\alpha_2 C_{200} + 4\alpha_1 C_{100}\left(1 - \cos q_z\right)\right) \\
&+ 16\alpha_1 C_{100}\left(1 - \frac{\cos q_x + \cos q_y}{2}\right)\left(1 - \cos q_z\right) \\
&= \left(1 - 14\alpha_1 C_{100} + 8\alpha_2 C_{110} + 2\alpha_2 C_{200}\right) \\
&\times \left(2 - \cos q_x - \cos q_y + 1 - \cos q_z\right) \\
&+ 16\alpha_1 C_{100}\left(1 - \frac{\cos q_x + \cos q_y}{2}\right)^2 + 4\alpha_1 C_{100}\left(1 - \cos q_z\right)^2 \\
&+ 16\alpha_1 C_{100}\left(1 - \frac{\cos q_x + \cos q_y}{2}\right)\left(1 - \cos q_z\right) \\
&= 3\left(1 - \gamma_{\mathbf{q}}\right)\left(1 - 14\alpha_1 C_{100} + 8\alpha_2 C_{110} + 2\alpha_2 C_{200}\right) \\
&+ 4\alpha_1 C_{100}\left(\left(2 - \cos q_x - \cos q_y\right)^2\right. \\
&\left. + 2\left(2 - \cos q_x - \cos q_y\right)\left(1 - \cos q_z\right) + \left(1 - \cos q_z\right)^2\right) \\
&= 3\left(1 - \gamma_{\mathbf{q}}\right) \\
&\times \left(1 - 14\alpha_1 C_{100} + 8\alpha_2 C_{110} + 2\alpha_2 C_{200}\right) + 36\alpha_1 C_{100}\left(1 - \gamma_{\mathbf{q}}\right)^2 \\
&= 3\left(1 - \gamma_{\mathbf{q}}\right) \\
&\times \left(1 + 10\alpha_1 C_{100} + 8\alpha_2 C_{110} + 2\alpha_2 C_{200} - 12\alpha_1 C_{100}\left(1 + \gamma_{\mathbf{q}}\right)\right). \quad (4.22)
\end{aligned}$$

Comparing Eqs. (4.1) and (4.22) we see that they coincide if

$$\eta_{100} \to \alpha_1, \quad \eta_{110} \to \alpha_2, \quad \eta_{200} \to \alpha_2. \quad (4.23)$$

Within the simplest assumption about the vertex parameters, $\eta_{100} = \eta_{110} = \eta_{200} = \eta$, Eq. (4.1) corresponds to the result of Ref. [12] with the same assumption about the vertex parameters: $\alpha_1 = \alpha_2 = \alpha$. We notice that this simple assumption yields $T_\mathrm{N} \approx 1.041$ whereas more sophisticated manipulation with the vertex parameters gives $T_\mathrm{N} \approx 1.079$ [12].

4.4. Comparison with high-temperature expansions and quantum Monte Carlo simulations

Simple cubic Heisenberg ferromagnet for arbitrary spin values $s \geq 1/2$ has been studied within high-temperature extrapolation techniques since the early sixties and a lot of results are available (see, e.g., Refs. [29,30]). Even more sophisticated high-temperature-series techniques, which are also applicable for more complicated quantum spin models, have been reported recently in Ref. [31]. The Curie temperature was estimated as $0.84|J|/k_\mathrm{B}$ already in 1967 [29] and confirmed later, e.g., in Ref. [30].

Quantum Monte Carlo simulations started in the late eighties. The simple-cubic-lattice spin-1/2 Heisenberg ferromagnet and antiferromagnet were examined many times in the past. The most recent data for the Curie temperature and the Néel temperature are:

$$k_{\rm B}T_{\rm C} = 0.839(1)|J|,$$
$$k_{\rm B}T_{\rm N} = 0.946(1)J, \qquad (4.24)$$

see Refs. [16–18]. This result agrees with earlier data from high-temperature expansions [29, 30].

We perform quantum Monte Carlo simulations using the ALPS package [19], namely, utilizing the application called the directed loop algorithm in the stochastic series expansion (SSE) representation (the `dirloop_sse` package). Using the directed loop SSE application we illustrate the temperature dependencies of various quantities. For the ferromagnetic case we examine the magnetization (per site) m, the static uniform susceptibility (per site) $\chi = \chi^{+-}_{\mathbf{q}=0,\omega=0} = 2\chi^{zz}_{\mathbf{q}=0,\omega=0}$, and the specific heat (per site) c. We set $J = -1$ and take $N = L^3$ sites with $L =$ 10, 20, 40, 80, 120. We put small symmetry-breaking uniform magnetic field $h = 10^{-4}$. Our findings are collected in Fig. 3. For the antiferromagnetic case we examine the temperature dependencies of the staggered (i.e., sublattice) magnetization (per site) m_s, the staggered static uniform susceptibility (per site) $\chi_s = \chi^{+-}_{\mathbf{q}=(\pi,\pi,\pi),\omega=0} = 2\chi^{zz}_{\mathbf{q}=(\pi,\pi,\pi),\omega=0}$, and the specific heat (per site) c. We set $J = 1$ and take $N = L^3$ sites with $L = 20$, 40, 80. Again we put small symmetry-breaking staggered (i.e., which has different signs on different sublattices) magnetic field $h_s = 10^{-4}$. Since the employed ALPS package does not yield $\chi^{zz}_{\mathbf{q}=(\pi,\pi,\pi),\omega=0}$, we find this quantity as the ratio $(m_s(h_{s2}) - m_s(h_{s1}))/(h_{s2} - h_{s1})$ with $h_{s2} = 10^{-4}$ and $h_{s1} = 0.5 \cdot 10^{-4}$. Our findings are collected in Fig. 4.

If one plots the thermodynamic quantities against T/T_c with the value of T_c as it is determined by the specific method, a discrepancy between the Green-function results and quantum Monte Carlo data (conditioned by different predictions for T_c) becomes hidden, see Fig. 5. [The quantum Monte Carlo estimate for T_c is obtained from the magnetization curve for the largest system size: We get $T_{\rm C} \approx 0.845$ and $T_{\rm N} \approx 0.975$ that is not far from more precise quantum Monte Carlo results, 0.839(1) and 0.946(1), reported in Tables 1 and 2, see also Eq. (4.24)].

In Fig. 6 we present the results for the magnetization as it follows after the Tyablikov approximation, see Eq. (3.2) (the ferromagnetic case) and Eq. (3.6) (the antiferromagnetic case). As Fig. 6 shows, the Tyablikov decoupling leads to reasonably good predictions for the magnetization, especially in the antiferromagnetic case.

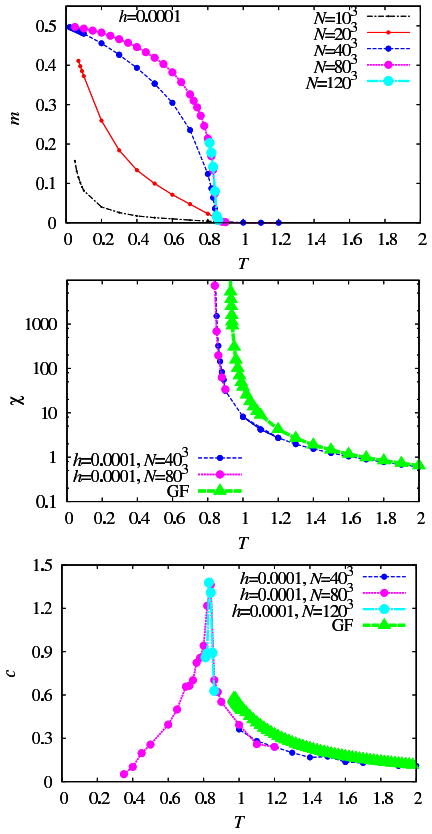

Figure 3. (Color online) Temperature dependence of the magnetization m, the static susceptibility χ, and the specific heat c for the spin-1/2 Heisenberg ferromagnet on a simple cubic lattice. Quantum Monte Carlo data are obtained for the system of different sizes 10^3, 20^3, 40^3, 80^3, 120^3 with $J = -1$ and $h = 10^{-4}$ (curves with circles). Green-function results are shown by (green) curves with up-triangles. The Curie temperature according to the reported quantum Monte Carlo simulations for magnetization curve of largest sizes is 0.845, whereas according to the Green-function method it is 0.926.

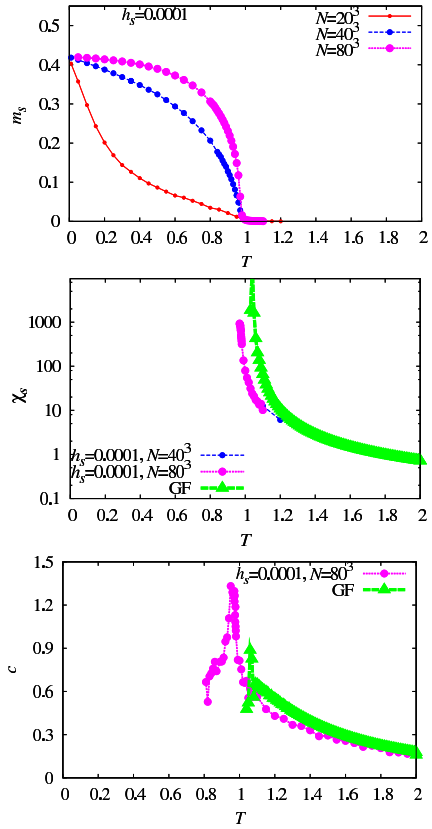

Figure 4. (Color online) Temperature dependence of the staggered magnetization m_s, the staggered static susceptibility χ_s, and the specific heat c for the spin-1/2 Heisenberg antiferromagnet on a simple cubic lattice. Quantum Monte Carlo data are obtained for the system of different sizes 20^3, 40^3, 80^3 with $J = 1$ and $h_s = 10^{-4}$ (curves with circles). Green-function results are shown by (green) curves with up-triangles. The Néel temperature according to the reported quantum Monte Carlo simulations for magnetization curve of largest sizes is 0.975, whereas according to the Green-function method it is 1.041.

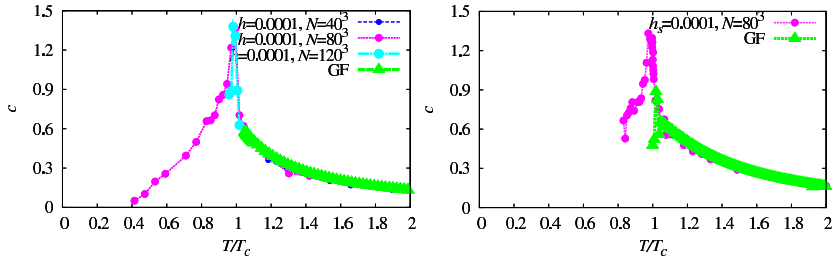

Figure 5. (Color online) Temperature dependence of the specific heat c for the spin-1/2 Heisenberg ferromagnet (left) and antiferromagnet (right) on a simple cubic lattice. These results were reported already in the corresponding panels of Figs. 3 and 4. Now we use for the quantum Monte Carlo simulations $T_c = 0.845$ (ferromagnet) and $T_c = 0.975$ (antiferromagnet), whereas for the Green-function results $T_c = 0.926$ (ferromagnet) and $T_c = 1.041$ (antiferromagnet).

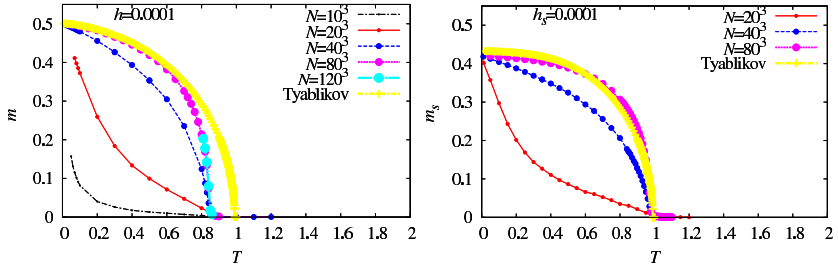

Figure 6. (Color online) Temperature dependence of the magnetization m for the spin-1/2 Heisenberg ferromagnet on a simple cubic lattice (left) and of the staggered magnetization m_s for the spin-1/2 Heisenberg antiferromagnet on a simple cubic lattice (right). Quantum Monte Carlo results were reported already in the corresponding panels of Figs. 3 and 4. Now we compare them to the results which follow after the Tyablikov approximation.

Let us make a few comments on the obtained temperature dependences. All approaches yield the value of $m_s(0) \approx 0.42$, see the corresponding panels in Fig. 4 and Fig. 6, which agrees with previous studies see, e.g., Ref. [32]. We notice that numerical differentiation in Eq. (4.15) produces a noise in the Green-function predictions for the dependence $c(T)$ while approaching T_c, see the corresponding panels in Figs. 3 and 4 and Fig. 5. Therefore, the Green-function predictions for the specific heat become less reliable around T_c.

Comparing the Green-function results with the benchmark quantum Monte Carlo data in Figs. 3 and 4, and in Fig. 5, one may conclude that in general, the agreement between both findings is quite reasonable.

5. Conclusions

To summarize, we have illustrated an application of the spin-rotation-invariant second-order Green-function method for studying the high-temperature properties of the spin-1/2 Heisenberg magnet on a simple cubic lattice with ferro- or antiferromagnetic nearest-neighbor interaction. The critical temperature T_c as it follows from the divergence of $\chi^{+-}_{\mathbf{q}=0,\omega=0}$ (for $J=-|J|<0$) or of $\chi^{+-}_{\mathbf{q}=(\pi,\pi,\pi),\omega=0}$ (for $J=|J|>0$) is in a reasonable agreement with quantum Monte Carlo and high-temperature expansions data. We intend to apply this approach for studying high-temperature properties in the presence of competing interaction (frustration).

Although we do not report new results, we believe the paper is valuable from methodological point of view, since it presents all details of calculations as well as comparisons with some other Green-function papers and numerics. Therefore it may be a good starting point for further attack of the high-temperature properties of frustrated quantum Heisenberg magnets.

Acknowledgments

The authors are grateful to J. Richter for many useful discussions and to P. Müller for critical reading of the manuscript. O. D. would like to thank the Abdus Salam International Centre for Theoretical Physics (Trieste, Italy) for partial support of these studies through the Senior Associate award.

A. Green function $\langle\langle s^+_{\mathbf{q}}; s^-_{\mathbf{q}}\rangle\rangle_\omega$ within the Kondo-Yamaji approximation

Let us elaborate in detail each term in Eqs. (2.4) and (2.5).

Consider the term $\mathrm{i}\hbar\langle[\dot{s}^+_{\mathbf{q}}, s^-_{\mathbf{q}}]_-\rangle$. Since

$$i\hbar\dot{s}^+_{\mathbf{q}} = \frac{1}{\sqrt{N}}\sum_{\mathbf{m}} e^{-\mathrm{i}\mathbf{q}\cdot\mathbf{m}}[s^+_{\mathbf{m}}, H]_- \tag{A.1}$$

and

$$\begin{aligned}[s^+_{\mathbf{m}}, H]_- = J\Big(&s^+_{m_x-1}s^z_{\mathbf{m}} + s^+_{m_y-1}s^z_{\mathbf{m}} + s^+_{m_z-1}s^z_{\mathbf{m}}\\ &-s^z_{m_x-1}s^+_{\mathbf{m}} - s^z_{m_y-1}s^+_{\mathbf{m}} - s^z_{m_z-1}s^+_{\mathbf{m}}\\ &+s^z_{\mathbf{m}}s^+_{m_x+1} + s^z_{\mathbf{m}}s^+_{m_y+1} + s^z_{\mathbf{m}}s^+_{m_z+1}\\ &-s^+_{\mathbf{m}}s^z_{m_x+1} - s^+_{\mathbf{m}}s^z_{m_y+1} - s^+_{\mathbf{m}}s^z_{m_z+1}\Big),\end{aligned} \tag{A.2}$$

we get

$$\begin{aligned}&\langle[\mathrm{i}\hbar\dot{s}^+_{\mathbf{q}}, s^-_{\mathbf{q}}]_-\rangle\\ &= \frac{J}{N}\sum_{\mathbf{m}}\langle -s^+_{m_x-1}s^-_{\mathbf{m}} - s^+_{m_y-1}s^-_{\mathbf{m}} - s^+_{m_z-1}s^-_{\mathbf{m}}\\ &\quad -2s^z_{m_x-1}s^z_{\mathbf{m}} - 2s^z_{m_y-1}s^z_{\mathbf{m}} - 2s^z_{m_z-1}s^z_{\mathbf{m}}\\ &\quad -s^-_{\mathbf{m}}s^+_{m_x+1} - s^-_{\mathbf{m}}s^+_{m_y+1} - s^-_{\mathbf{m}}s^+_{m_z+1}\\ &\quad -2s^z_{\mathbf{m}}s^z_{m_x+1} - 2s^z_{\mathbf{m}}s^z_{m_y+1} - 2s^z_{\mathbf{m}}s^z_{m_z+1}\\ &\quad +2e^{-\mathrm{i}q_x}s^z_{m_x-1}s^z_{\mathbf{m}} + 2e^{-\mathrm{i}q_y}s^z_{m_y-1}s^z_{\mathbf{m}} + 2e^{-\mathrm{i}q_z}s^z_{m_z-1}s^z_{\mathbf{m}}\\ &\quad +e^{-\mathrm{i}q_x}s^-_{m_x-1}s^+_{\mathbf{m}} + e^{-\mathrm{i}q_y}s^-_{m_y-1}s^+_{\mathbf{m}} + e^{-\mathrm{i}q_z}s^-_{m_z-1}s^+_{\mathbf{m}}\\ &\quad +2e^{\mathrm{i}q_x}s^z_{\mathbf{m}}s^z_{m_x+1} + 2e^{\mathrm{i}q_y}s^z_{\mathbf{m}}s^z_{m_y+1} + 2e^{\mathrm{i}q_z}s^z_{\mathbf{m}}s^z_{m_z+1}\\ &\quad +e^{\mathrm{i}q_x}s^+_{\mathbf{m}}s^-_{m_x+1} + e^{\mathrm{i}q_y}s^+_{\mathbf{m}}s^-_{m_y+1} + e^{\mathrm{i}q_z}s^+_{\mathbf{m}}s^-_{m_z+1}\rangle.\end{aligned} \tag{A.3}$$

Because of translational invariance we have $\sum_{\mathbf{m}}(\ldots) = N$ and $C_{100} = \langle s^+_{m_x-1}s^-_{\mathbf{m}}\rangle = C_{010} = \langle s^+_{m_y-1}s^-_{\mathbf{m}}\rangle$ etc., $B_{100} = \langle s^z_{m_x-1}s^z_{\mathbf{m}}\rangle = B_{010} = \langle s^z_{m_y-1}s^z_{\mathbf{m}}\rangle$ etc.. Because of rotational invariance we have $B = C/2$. Therefore

$$\begin{aligned}\langle[\mathrm{i}\hbar\dot{s}^+_{\mathbf{q}}, s^-_{\mathbf{q}}]_-\rangle &= M_{\mathbf{q}},\\ M_{\mathbf{q}} &= 4JC_{100}\left(\cos q_x + \cos q_y + \cos q_z - 3\right).\end{aligned} \tag{A.4}$$

We pass to the term $-\hbar^2\langle\langle \ddot{s}^+_{\mathbf{q}}; s^-_{\mathbf{q}}\rangle\rangle_\omega$ in Eq. (2.5). Since

$$-\hbar^2\ddot{s}^+_{\mathbf{q}} = \frac{J}{\sqrt{N}}\sum_{\mathbf{m}} e^{-\mathrm{i}\mathbf{q}\cdot\mathbf{m}}$$
$$\times\Big([s^+_{m_x-1}s^z_{\mathbf{m}}, H]_- + [s^+_{m_y-1}s^z_{\mathbf{m}}, H]_- + [s^+_{m_z-1}s^z_{\mathbf{m}}, H]_-$$
$$-[s^z_{m_x-1}s^+_{\mathbf{m}}, H]_- - [s^z_{m_y-1}s^+_{\mathbf{m}}, H]_- - [s^z_{m_z-1}s^+_{\mathbf{m}}, H]_-$$
$$+[s^z_{\mathbf{m}}s^+_{m_x+1}, H]_- + [s^z_{\mathbf{m}}s^+_{m_y+1}, H]_- + [s^z_{\mathbf{m}}s^+_{m_z+1}, H]_-$$
$$-[s^+_{\mathbf{m}}s^z_{m_x+1}, H]_- - [s^+_{\mathbf{m}}s^z_{m_y+1}, H]_- - [s^+_{\mathbf{m}}s^z_{m_z+1}, H]_-\Big), \qquad (A.5)$$

we must calculate first $[s^+_{\mathbf{m}'}s^z_{\mathbf{m}}, H]_-$. We get

$$\frac{1}{J}[s^+_{\mathbf{m}'}s^z_{\mathbf{m}}, H]_- = \frac{1}{2}\left(s^+_{\mathbf{m}'}s^+_{\mathbf{m}}s^-_{m_x+1} - s^+_{\mathbf{m}'}s^-_{\mathbf{m}}s^+_{m_x+1}\right)$$
$$+\frac{1}{2}\left(-s^+_{\mathbf{m}'}s^+_{m_x-1}s^-_{\mathbf{m}} + s^+_{\mathbf{m}'}s^-_{m_x-1}s^+_{\mathbf{m}}\right)$$
$$+s^z_{\mathbf{m}'}s^+_{m'_x+1}s^z_{\mathbf{m}} + s^+_{m'_x-1}s^z_{\mathbf{m}'}s^z_{\mathbf{m}}$$
$$-s^+_{\mathbf{m}'}s^z_{m'_x+1}s^z_{\mathbf{m}} - s^z_{m'_x-1}s^+_{\mathbf{m}'}s^z_{\mathbf{m}}$$
$$+\frac{1}{2}\left(s^+_{\mathbf{m}'}s^+_{\mathbf{m}}s^-_{m_y+1} - s^+_{\mathbf{m}'}s^-_{\mathbf{m}}s^+_{m_y+1}\right)$$
$$+\frac{1}{2}\left(-s^+_{\mathbf{m}'}s^+_{m_y-1}s^-_{\mathbf{m}} + s^+_{\mathbf{m}'}s^-_{m_y-1}s^+_{\mathbf{m}}\right)$$
$$+s^z_{\mathbf{m}'}s^+_{m'_y+1}s^z_{\mathbf{m}} + s^+_{m'_y-1}s^z_{\mathbf{m}'}s^z_{\mathbf{m}}$$
$$-s^+_{\mathbf{m}'}s^z_{m'_y+1}s^z_{\mathbf{m}} - s^z_{m'_y-1}s^+_{\mathbf{m}'}s^z_{\mathbf{m}}$$
$$+\frac{1}{2}\left(s^+_{\mathbf{m}'}s^+_{\mathbf{m}}s^-_{m_z+1} - s^+_{\mathbf{m}'}s^-_{\mathbf{m}}s^+_{m_z+1}\right)$$
$$+\frac{1}{2}\left(-s^+_{\mathbf{m}'}s^+_{m_z-1}s^-_{\mathbf{m}} + s^+_{\mathbf{m}'}s^-_{m_z-1}s^+_{\mathbf{m}}\right)$$
$$+s^z_{\mathbf{m}'}s^+_{m'_z+1}s^z_{\mathbf{m}} + s^+_{m'_z-1}s^z_{\mathbf{m}'}s^z_{\mathbf{m}}$$
$$-s^+_{\mathbf{m}'}s^z_{m'_z+1}s^z_{\mathbf{m}} - s^z_{m'_z-1}s^+_{\mathbf{m}'}s^z_{\mathbf{m}}. \qquad (A.6)$$

Now we can proceed with the r.h.s. of Eq. (A.5). We begin with the first three terms in the r.h.s. of Eq. (A.5). Let us write down the contribution of the first term in the r.h.s. of Eq. (A.5) (i.e., of the one which contains $[s^+_{m_x-1}s^z_{\mathbf{m}}, H]_-$) to $-\hbar^2\langle\langle \ddot{s}^+_{\mathbf{q}}; s^-_{\mathbf{q}}\rangle\rangle_\omega$:

$$\frac{J^2}{N}\sum_{\mathbf{m}}\sum_{\mathbf{g}} e^{\mathrm{i}\mathbf{q}\cdot(\mathbf{g}-\mathbf{m})}$$

$$\times\left(\frac{1}{2}\langle\langle s^+_{m_x-1}s^+_{\mathbf{m}}s^-_{m_x+1}; s^-_{\mathbf{g}}\rangle\rangle_\omega - \frac{1}{2}\langle\langle s^+_{m_x-1}s^-_{\mathbf{m}}s^+_{m_x+1}; s^-_{\mathbf{g}}\rangle\rangle_\omega\right.$$
$$-0 + \frac{1}{2}\langle\langle\left(\frac{1}{2} + s^z_{m_x-1}\right)s^+_{\mathbf{m}}; s^-_{\mathbf{g}}\rangle\rangle_\omega$$
$$+\langle\langle s^z_{m_x-1}\left(-\frac{1}{2}s^+_{\mathbf{m}}\right); s^-_{\mathbf{g}}\rangle\rangle_\omega + \langle\langle s^+_{m_x-2}s^z_{m_x-1}s^z_{\mathbf{m}}; s^-_{\mathbf{g}}\rangle\rangle_\omega$$
$$-\frac{1}{4}\langle\langle s^+_{m_x-1}; s^-_{\mathbf{g}}\rangle\rangle_\omega - \langle\langle s^z_{m_x-2}s^+_{m_x-1}s^z_{\mathbf{m}}; s^-_{\mathbf{g}}\rangle\rangle_\omega$$
$$+\frac{1}{2}\langle\langle s^+_{m_x-1}s^+_{\mathbf{m}}s^-_{m_y+1}; s^-_{\mathbf{g}}\rangle\rangle_\omega - \frac{1}{2}\langle\langle s^+_{m_x-1}s^-_{\mathbf{m}}s^+_{m_y+1}; s^-_{\mathbf{g}}\rangle\rangle_\omega$$
$$-\frac{1}{2}\langle\langle s^+_{m_x-1}s^+_{m_y-1}s^-_{\mathbf{m}}; s^-_{\mathbf{g}}\rangle\rangle_\omega + \frac{1}{2}\langle\langle s^+_{m_x-1}s^-_{m_y-1}s^+_{\mathbf{m}}; s^-_{\mathbf{g}}\rangle\rangle_\omega$$
$$+\langle\langle s^z_{m_x-1}s^+_{m_x-1,m_y+1}s^z_{\mathbf{m}}; s^-_{\mathbf{g}}\rangle\rangle_\omega + \langle\langle s^+_{m_x-1,m_y-1}s^z_{m_x-1}s^z_{\mathbf{m}}; s^-_{\mathbf{g}}\rangle\rangle_\omega$$
$$-\langle\langle s^+_{m_x-1}s^z_{m_x-1,m_y+1}s^z_{\mathbf{m}}; s^-_{\mathbf{g}}\rangle\rangle_\omega - \langle\langle s^z_{m_x-1,m_y-1}s^+_{m_x-1}s^z_{\mathbf{m}}; s^-_{\mathbf{g}}\rangle\rangle_\omega$$
$$+\frac{1}{2}\langle\langle s^+_{m_x-1}s^+_{\mathbf{m}}s^-_{m_z+1}; s^-_{\mathbf{g}}\rangle\rangle_\omega - \frac{1}{2}\langle\langle s^+_{m_x-1}s^-_{\mathbf{m}}s^+_{m_z+1}; s^-_{\mathbf{g}}\rangle\rangle_\omega$$
$$-\frac{1}{2}\langle\langle s^+_{m_x-1}s^+_{m_z-1}s^-_{\mathbf{m}}; s^-_{\mathbf{g}}\rangle\rangle_\omega + \frac{1}{2}\langle\langle s^+_{m_x-1}s^-_{m_z-1}s^+_{\mathbf{m}}; s^-_{\mathbf{g}}\rangle\rangle_\omega$$
$$+\langle\langle s^z_{m_x-1}s^+_{m_x-1,m_z+1}s^z_{\mathbf{m}}; s^-_{\mathbf{g}}\rangle\rangle_\omega + \langle\langle s^+_{m_x-1,m_z-1}s^z_{m_x-1}s^z_{\mathbf{m}}; s^-_{\mathbf{g}}\rangle\rangle_\omega$$
$$\left.-\langle\langle s^+_{m_x-1}s^z_{m_x-1,m_z+1}s^z_{\mathbf{m}}; s^-_{\mathbf{g}}\rangle\rangle_\omega - \langle\langle s^z_{m_x-1,m_z-1}s^+_{m_x-1}s^z_{\mathbf{m}}; s^-_{\mathbf{g}}\rangle\rangle_\omega\right). \qquad (A.7)$$

We have used the following exact on-site relations: $s^+s^+ = 0$, $s^+s^- = 1/2 + s^z$, $s^+s^z = -s^+/2$, and $s^zs^z = 1/4$. Next we have to use the Kondo-Yamaji decoupling (2.6). As a result, Eq. (A.7) becomes

$$\frac{J^2}{N}\sum_{\mathbf{m}}\sum_{\mathbf{g}} e^{\mathrm{i}\mathbf{q}\cdot(\mathbf{g}-\mathbf{m})}$$
$$\times\left(\frac{1}{2}\eta_{200}C_{200}\langle\langle s^+_{\mathbf{m}}; s^-_{\mathbf{g}}\rangle\rangle_\omega - \frac{1}{2}\eta_{100}C_{100}\langle\langle s^+_{m_x+1}; s^-_{\mathbf{g}}\rangle\rangle_\omega\right.$$
$$+\frac{1}{4}\langle\langle s^+_{\mathbf{m}}; s^-_{\mathbf{g}}\rangle\rangle_\omega$$
$$+\frac{1}{2}\eta_{100}C_{100}\langle\langle s^+_{m_x-2}; s^-_{\mathbf{g}}\rangle\rangle_\omega$$
$$-\frac{1}{4}\langle\langle s^+_{m_x-1}; s^-_{\mathbf{g}}\rangle\rangle_\omega - \frac{1}{2}\eta_{200}C_{200}\langle\langle s^+_{m_x-1}; s^-_{\mathbf{g}}\rangle\rangle_\omega$$
$$+\frac{1}{2}\eta_{110}C_{110}\langle\langle s^+_{\mathbf{m}}; s^-_{\mathbf{g}}\rangle\rangle_\omega - \frac{1}{2}\eta_{100}C_{100}\langle\langle s^+_{m_y+1}; s^-_{\mathbf{g}}\rangle\rangle_\omega$$
$$\left.-\frac{1}{2}\eta_{100}C_{100}\langle\langle s^+_{m_y-1}; s^-_{\mathbf{g}}\rangle\rangle_\omega + \frac{1}{2}\eta_{110}C_{110}\langle\langle s^+_{\mathbf{m}}; s^-_{\mathbf{g}}\rangle\rangle_\omega\right.$$

$$+\frac{1}{2}\eta_{100}C_{100}\langle\langle s^+_{m_x-1,m_y+1};s^-_{\mathbf{g}}\rangle\rangle_\omega+\frac{1}{2}\eta_{100}C_{100}\langle\langle s^+_{m_x-1,m_y-1};s^-_{\mathbf{g}}\rangle\rangle_\omega$$
$$-\frac{1}{2}\eta_{110}C_{110}\langle\langle s^+_{m_x-1};s^-_{\mathbf{g}}\rangle\rangle_\omega-\frac{1}{2}\eta_{110}C_{110}\langle\langle s^+_{m_x-1};s^-_{\mathbf{g}}\rangle\rangle_\omega$$
$$+\frac{1}{2}\eta_{101}C_{101}\langle\langle s^+_{\mathbf{m}};s^-_{\mathbf{g}}\rangle\rangle_\omega-\frac{1}{2}\eta_{100}C_{100}\langle\langle s^+_{m_z+1};s^-_{\mathbf{g}}\rangle\rangle_\omega$$
$$-\frac{1}{2}\eta_{100}C_{100}\langle\langle s^+_{m_z-1};s^-_{\mathbf{g}}\rangle\rangle_\omega+\frac{1}{2}\eta_{101}C_{101}\langle\langle s^+_{\mathbf{m}};s^-_{\mathbf{g}}\rangle\rangle_\omega$$
$$+\frac{1}{2}\eta_{100}C_{100}\langle\langle s^+_{m_x-1,m_z+1};s^-_{\mathbf{g}}\rangle\rangle_\omega+\frac{1}{2}\eta_{100}C_{100}\langle\langle s^+_{m_x-1,m_z-1};s^-_{\mathbf{g}}\rangle\rangle_\omega$$
$$-\frac{1}{2}\eta_{101}C_{101}\langle\langle s^+_{m_x-1};s^-_{\mathbf{g}}\rangle\rangle_\omega-\frac{1}{2}\eta_{101}C_{101}\langle\langle s^+_{m_x-1};s^-_{\mathbf{g}}\rangle\rangle_\omega\Bigg). \quad (A.8)$$

We have to do similar calculations for the second and the third terms in the r.h.s. of Eq. (A.5). Combining these findings, we get for the first three terms in the r.h.s. of Eq. (A.5) the following result:

$$\frac{-\hbar^2\langle\langle \ddot{s}^+_{\mathbf{q}};s^-_{\mathbf{q}}\rangle\rangle_\omega}{J^2\langle\langle s^+_{\mathbf{q}};s^-_{\mathbf{q}}\rangle\rangle_\omega}$$
$$=\frac{1}{2}\eta_{200}C_{200}+\frac{1}{4}+\eta_{110}C_{110}+\eta_{101}C_{101}$$
$$+\eta_{110}C_{110}+\frac{1}{2}\eta_{020}C_{020}+\frac{1}{4}+\eta_{011}C_{011}$$
$$+\eta_{101}C_{101}+\eta_{011}C_{011}+\frac{1}{2}\eta_{002}C_{002}+\frac{1}{4}$$
$$-\left(\eta_{010}C_{010}+\eta_{001}C_{001}\right)\cos q_x$$
$$-\frac{1}{2}\eta_{100}C_{100}e^{\mathrm{i}q_x}$$
$$+\Bigg(-\frac{1}{4}-\frac{1}{2}\eta_{200}C_{200}-\eta_{110}C_{110}-\eta_{101}C_{101}$$
$$+\eta_{100}C_{100}\cos q_y+\eta_{100}C_{100}\cos q_z\Bigg)e^{-\mathrm{i}q_x}$$
$$-\left(\eta_{100}C_{100}+\eta_{001}C_{001}\right)\cos q_y$$
$$-\frac{1}{2}\eta_{010}C_{010}e^{\mathrm{i}q_y}$$
$$+\Bigg(-\eta_{110}C_{110}-\frac{1}{4}-\frac{1}{2}\eta_{020}C_{020}-\eta_{011}C_{011}$$
$$+\eta_{010}C_{010}\cos q_x+\eta_{010}C_{010}\cos q_z\Bigg)e^{-\mathrm{i}q_y}$$
$$-\left(\eta_{100}C_{100}+\eta_{010}C_{010}\right)\cos q_z$$
$$-\frac{1}{2}\eta_{001}C_{001}e^{\mathrm{i}q_z}$$

$$+\Bigg(-\eta_{101}C_{101}-\eta_{011}C_{011}-\frac{1}{4}-\frac{1}{2}\eta_{002}C_{002}$$
$$+\eta_{001}C_{001}\cos q_x+\eta_{001}C_{001}\cos q_y\Bigg)e^{-\mathrm{i}q_z}$$
$$+\frac{1}{2}\eta_{100}C_{100}e^{-2\mathrm{i}q_x}+\frac{1}{2}\eta_{010}C_{010}e^{-2\mathrm{i}q_y}+\frac{1}{2}\eta_{001}C_{001}e^{-2\mathrm{i}q_z}. \quad (A.9)$$

Next three terms (the second three terms) in the r.h.s. of Eq. (A.5) give the same result as in Eq. (A.9). Furthermore, the third three terms and the fourth three terms in the r.h.s. of Eq. (A.5) yield complex conjugate expression of that one which is given in Eq. (A.9). We can simplify our formulas using the consequences of translational invariance: $C_{100}=C_{010}=C_{001}$, $C_{110}=C_{011}=C_{101}$ etc. Therefore, after tedious but doable calculations we have arrived at the final formula for the Green function $\langle\langle s^+_{\mathbf{q}};s^-_{\mathbf{q}}\rangle\rangle_\omega$.

The final result for the Green function $\langle\langle s^+_{\mathbf{q}};s^-_{\mathbf{q}}\rangle\rangle_\omega$ within the adopted approximation (2.6) reads:

$$\langle\langle s^+_{\mathbf{q}};s^-_{\mathbf{q}}\rangle\rangle_\omega=\frac{M_{\mathbf{q}}}{(\hbar\omega)^2-(\hbar\omega_{\mathbf{q}})^2}, \quad (A.10)$$

where

$$M_{\mathbf{q}}=4JC_{100}\left(\cos q_x+\cos q_y+\cos q_z-3\right) \quad (A.11)$$

and

$$\left(\frac{\hbar\omega_{\mathbf{q}}}{J}\right)^2=3+24\eta_{110}C_{110}+6\eta_{200}C_{200}$$
$$-\left(1+10\eta_{100}C_{100}+8\eta_{110}C_{110}+2\eta_{200}C_{200}\right)$$
$$\times\left(\cos q_x+\cos q_y+\cos q_z\right)$$
$$+8\eta_{100}C_{100}$$
$$\times\left(\cos q_x\cos q_y+\cos q_x\cos q_z+\cos q_y\cos q_z\right)$$
$$+2\eta_{100}C_{100}\left(\cos(2q_x)+\cos(2q_y)+\cos(2q_z)\right). \quad (A.12)$$

We may rewrite to obtained result even in a more convenient form. After introducing

$$-1\le\gamma_{\mathbf{q}}=\frac{1}{3}\left(\cos q_x+\cos q_y+\cos q_z\right)\le 1, \quad (A.13)$$

we have instead of Eqs. (A.11) and (A.12) the following formulas

$$M_{\mathbf{q}}=-12JC_{100}\left(1-\gamma_{\mathbf{q}}\right) \quad (A.14)$$

and

$$\left(\frac{\hbar\omega_{\mathbf{q}}}{J}\right)^2 = 3\left(1-\gamma_{\mathbf{q}}\right)\left(1+10\eta_{100}C_{100}\right.$$
$$\left.+8\eta_{110}C_{110}+2\eta_{200}C_{200}-12\eta_{100}C_{100}\left(1+\gamma_{\mathbf{q}}\right)\right), \qquad \text{(A.15)}$$

respectively [cf. Eq. (4.1)].

B. η, C_{100}, C_{110}, and C_{200} in the high-temperature limit

In the high-temperature limit $T\to\infty$, Eq. (4.4) becomes

$$\langle s^-_{\mathbf{q}} s^+_{\mathbf{q}}\rangle = \frac{M_{\mathbf{q}}}{2\hbar\omega_{\mathbf{q}}}\left(1+\frac{2}{e^{\frac{\hbar\omega_{\mathbf{q}}}{T}}-1}\right)$$
$$= \frac{M_{\mathbf{q}}}{2\hbar\omega_{\mathbf{q}}}\left(1+\frac{2}{1+\frac{\hbar\omega_{\mathbf{q}}}{T}+\ldots-1}\right)$$
$$\to \frac{M_{\mathbf{q}}}{\left(\hbar\omega_{\mathbf{q}}\right)^2}T =$$
$$\frac{-12C_{100}\left(1-\gamma_{\mathbf{q}}\right)}{3\left(1-\gamma_{\mathbf{q}}\right)\left(1+10\eta C_{100}+8\eta C_{110}+2\eta C_{200}-12\eta C_{100}\left(1+\gamma_{\mathbf{q}}\right)\right)}\frac{T}{J}$$
$$= \frac{-4C_{100}}{1+10\eta C_{100}+8\eta C_{110}+2\eta C_{200}-12\eta C_{100}\left(1+\gamma_{\mathbf{q}}\right)}\frac{T}{J} \qquad \text{(B.1)}$$

and the equations to be solved [see Eqs. (4.7), (4.8)] read:

$$\frac{1}{2} = \frac{1}{(2\pi)^3}\int_{-\pi}^{\pi}\mathrm{d}q_x\int_{-\pi}^{\pi}\mathrm{d}q_y\int_{-\pi}^{\pi}\mathrm{d}q_z\langle s^-_{\mathbf{q}} s^+_{\mathbf{q}}\rangle$$
$$= \frac{1}{(2\pi)^3}\int_{-\pi}^{\pi}\mathrm{d}q_x\int_{-\pi}^{\pi}\mathrm{d}q_y\int_{-\pi}^{\pi}\mathrm{d}q_z$$
$$\times\frac{-4C_{100}}{1+10\eta C_{100}+8\eta C_{110}+2\eta C_{200}-12\eta C_{100}\left(1+\gamma_{\mathbf{q}}\right)}\frac{T}{J}, \qquad \text{(B.2)}$$

$$C_{100} = \frac{1}{(2\pi)^3}\int_{-\pi}^{\pi}\mathrm{d}q_x\int_{-\pi}^{\pi}\mathrm{d}q_y\int_{-\pi}^{\pi}\mathrm{d}q_z e^{\mathrm{i}q_x}\langle s^-_{\mathbf{q}} s^+_{\mathbf{q}}\rangle$$
$$= \frac{1}{(2\pi)^3}\int_{-\pi}^{\pi}\mathrm{d}q_x\int_{-\pi}^{\pi}\mathrm{d}q_y\int_{-\pi}^{\pi}\mathrm{d}q_z\cos q_x$$
$$\times\frac{-4C_{100}}{1+10\eta C_{100}+8\eta C_{110}+2\eta C_{200}-12\eta C_{100}\left(1+\gamma_{\mathbf{q}}\right)}\frac{T}{J}, \qquad \text{(B.3)}$$

$$C_{110} = \frac{1}{(2\pi)^3}\int_{-\pi}^{\pi}\mathrm{d}q_x\int_{-\pi}^{\pi}\mathrm{d}q_y\int_{-\pi}^{\pi}\mathrm{d}q_z e^{\mathrm{i}(q_x+q_y)}\langle s^-_{\mathbf{q}} s^+_{\mathbf{q}}\rangle$$
$$= \frac{1}{(2\pi)^3}\int_{-\pi}^{\pi}\mathrm{d}q_x\int_{-\pi}^{\pi}\mathrm{d}q_y\int_{-\pi}^{\pi}\mathrm{d}q_z\cos q_x\cos q_y$$
$$\times\frac{-4C_{100}}{1+10\eta C_{100}+8\eta C_{110}+2\eta C_{200}-12\eta C_{100}\left(1+\gamma_{\mathbf{q}}\right)}\frac{T}{J}, \qquad \text{(B.4)}$$

$$C_{200} = \frac{1}{(2\pi)^3}\int_{-\pi}^{\pi}\mathrm{d}q_x\int_{-\pi}^{\pi}\mathrm{d}q_y\int_{-\pi}^{\pi}\mathrm{d}q_z e^{2\mathrm{i}q_x}\langle s^-_{\mathbf{q}} s^+_{\mathbf{q}}\rangle$$
$$= \frac{1}{(2\pi)^3}\int_{-\pi}^{\pi}\mathrm{d}q_x\int_{-\pi}^{\pi}\mathrm{d}q_y\int_{-\pi}^{\pi}\mathrm{d}q_z\cos(2q_x)$$
$$\times\frac{-4C_{100}}{1+10\eta C_{100}+8\eta C_{110}+2\eta C_{200}-12\eta C_{100}\left(1+\gamma_{\mathbf{q}}\right)}\frac{T}{J}. \qquad \text{(B.5)}$$

We look for the first nonvanishing terms in $|J|/T$. Assume that

$$C_{100} = \frac{A}{T^\alpha}, \quad C_{110} = \frac{B}{T^\beta}, \quad C_{200} = \frac{C}{T^\gamma}, \quad \eta = D. \qquad \text{(B.6)}$$

Then Eq. (B.2) immediately yields

$$C_{100} = -\frac{1}{8}\frac{J}{T}. \qquad \text{(B.7)}$$

Furthermore, Eq. (B.3) reads

$$1 = \frac{1}{(2\pi)^3}\int_{-\pi}^{\pi}\mathrm{d}q_x\int_{-\pi}^{\pi}\mathrm{d}q_y\int_{-\pi}^{\pi}\mathrm{d}q_z\cos q_x\times$$
$$\frac{-4}{\left(1+10\eta C_{100}+8\eta C_{110}+2\eta C_{200}\right)\left(1-\frac{12\eta C_{100}\left(1+\gamma_{\mathbf{q}}\right)}{1+10\eta C_{100}+8\eta C_{110}+2\eta C_{200}}\right)}\frac{T}{J}$$
$$= \frac{1}{(2\pi)^3}\int_{-\pi}^{\pi}\mathrm{d}q_x\int_{-\pi}^{\pi}\mathrm{d}q_y\int_{-\pi}^{\pi}\mathrm{d}q_z\cos q_x$$
$$\times\frac{-4}{1+10\eta C_{100}+8\eta C_{110}+2\eta C_{200}}$$
$$\times\left(1+\frac{12\eta C_{100}\left(1+\gamma_{\mathbf{q}}\right)}{1+10\eta C_{100}+8\eta C_{110}+2\eta C_{200}}+\ldots\right)\frac{T}{J}. \qquad \text{(B.8)}$$

We have used already the assumptions (B.6): The term which contains $(1+\gamma_{\mathbf{q}})$ is small with respect to 1. Furthermore,

$$1 = \frac{1}{(2\pi)^3}\int_{-\pi}^{\pi}\mathrm{d}q_x\int_{-\pi}^{\pi}\mathrm{d}q_y\int_{-\pi}^{\pi}\mathrm{d}q_z\cos q_x\frac{T}{J}\times$$

$$\frac{-48\eta C_{100}}{\left(1+10\eta C_{100}+8\eta C_{110}+2\eta C_{200}\right)^2}\left(1+\frac{\cos q_x+\cos q_y+\cos q_z}{3}\right)$$
$$=\frac{-48\eta C_{100}}{\left(1+10\eta C_{100}+8\eta C_{110}+2\eta C_{200}\right)^2}\frac{1}{2\pi}\int_{-\pi}^{\pi}\mathrm{d}q_x\frac{\cos^2 q_x}{3}\frac{T}{J}$$
$$=\frac{-16\eta C_{100}}{\left(1+10\eta C_{100}+8\eta C_{110}+2\eta C_{200}\right)^2}\frac{1}{2\pi}\int_{-\pi}^{\pi}\mathrm{d}q_x\frac{1+\cos(2q_x)}{2}\frac{T}{J}$$
$$=\frac{-8\eta C_{100}}{\left(1+10\eta C_{100}+8\eta C_{110}+2\eta C_{200}\right)^2}\frac{T}{J}$$
$$=\frac{\eta}{\left(1+10\eta C_{100}+8\eta C_{110}+2\eta C_{200}\right)^2}\to\eta. \quad \text{(B.9)}$$

Hence

$$\eta=1. \quad \text{(B.10)}$$

In fact, owing to Eq. (B.7), we were considering the following equation:

$$2C_{100}=\frac{1}{(2\pi)^3}\int_{-\pi}^{\pi}\mathrm{d}q_x\int_{-\pi}^{\pi}\mathrm{d}q_y\int_{-\pi}^{\pi}\mathrm{d}q_z\cos q_x\frac{1}{1+\frac{3}{2}\eta\frac{J}{T}\left(1+\gamma_{\mathbf{q}}\right)}$$
$$=\frac{1}{(2\pi)^3}\int_{-\pi}^{\pi}\mathrm{d}q_x\int_{-\pi}^{\pi}\mathrm{d}q_y\int_{-\pi}^{\pi}\mathrm{d}q_z\cos q_x$$
$$\times\left(1-\frac{3}{2}\eta\frac{J}{T}\left(1+\gamma_{\mathbf{q}}\right)+\frac{9}{4}\eta^2\left(\frac{J}{T}\right)^2\left(1+\gamma_{\mathbf{q}}\right)^2+\ldots\right)$$
$$=\frac{1}{2\pi}\int_{-\pi}^{\pi}\mathrm{d}q_x\cos q_x\left(-\frac{3}{2}\eta\frac{J}{T}\frac{\cos q_x}{3}\right)$$
$$=-\frac{3}{2}\eta\frac{J}{T}\frac{1}{3}\frac{1}{2}=-\frac{1}{4}\eta\frac{J}{T}, \quad \text{(B.11)}$$

which gives $\eta=1$.

Similarly for C_{110} and C_{200} (and another correlation functions) we should rewrite Eqs. (B.4) and (B.5) as follows:

$$2C_{110}=\frac{1}{(2\pi)^3}\int_{-\pi}^{\pi}\mathrm{d}q_x\int_{-\pi}^{\pi}\mathrm{d}q_y\int_{-\pi}^{\pi}\mathrm{d}q_z\cos q_x\cos q_y\frac{1}{1+\frac{3}{2}\frac{J}{T}\left(1+\gamma_{\mathbf{q}}\right)}$$
$$=\frac{1}{(2\pi)^3}\int_{-\pi}^{\pi}\mathrm{d}q_x\int_{-\pi}^{\pi}\mathrm{d}q_y\int_{-\pi}^{\pi}\mathrm{d}q_z\cos q_x\cos q_y$$
$$\times\left(1-\frac{3}{2}\frac{J}{T}\left(1+\gamma_{\mathbf{q}}\right)+\frac{9}{4}\left(\frac{J}{T}\right)^2\left(1+\gamma_{\mathbf{q}}\right)^2+\ldots\right)$$

$$=\frac{1}{(2\pi)^2}\int_{-\pi}^{\pi}\mathrm{d}q_x\int_{-\pi}^{\pi}\mathrm{d}q_y\cos^2 q_x\cos^2 q_y\frac{9}{4}\left(\frac{J}{T}\right)^2\frac{2}{9}$$
$$=\frac{1}{4}\frac{9}{4}\left(\frac{J}{T}\right)^2\frac{2}{9}=\frac{1}{8}\left(\frac{J}{T}\right)^2; \quad \text{(B.12)}$$

hence

$$C_{110}=\frac{1}{16}\left(\frac{J}{T}\right)^2; \quad \text{(B.13)}$$

$$2C_{200}=\frac{1}{(2\pi)^3}\int_{-\pi}^{\pi}\mathrm{d}q_x\int_{-\pi}^{\pi}\mathrm{d}q_y\int_{-\pi}^{\pi}\mathrm{d}q_z\cos\left(2q_x\right)\frac{1}{1+\frac{3}{2}\frac{J}{T}\left(1+\gamma_{\mathbf{q}}\right)}$$
$$=\frac{1}{(2\pi)^3}\int_{-\pi}^{\pi}\mathrm{d}q_x\int_{-\pi}^{\pi}\mathrm{d}q_y\int_{-\pi}^{\pi}\mathrm{d}q_z\cos\left(2q_x\right)$$
$$\times\left(1-\frac{3}{2}\frac{J}{T}\left(1+\gamma_{\mathbf{q}}\right)+\frac{9}{4}\left(\frac{J}{T}\right)^2\left(1+\gamma_{\mathbf{q}}\right)^2+\ldots\right)$$
$$=\frac{1}{2\pi}\int_{-\pi}^{\pi}\mathrm{d}q_x\cos\left(2q_x\right)\frac{9}{4}\left(\frac{J}{T}\right)^2\frac{1}{18}\cos\left(2q_x\right)$$
$$=\frac{1}{8}\left(\frac{J}{T}\right)^2\frac{1}{2}=\frac{1}{16}\left(\frac{J}{T}\right)^2; \quad \text{(B.14)}$$

hence

$$C_{200}=\frac{1}{32}\left(\frac{J}{T}\right)^2. \quad \text{(B.15)}$$

Thus, in the high-temperature limit the unknown quantities should behave as follows:

$$\eta=1+o(1),$$
$$C_{100}=-\frac{1}{8}\frac{J}{T}+o\left(\frac{J}{T}\right),$$
$$C_{110}=\frac{1}{16}\left(\frac{J}{T}\right)^2+o\left(\left(\frac{J}{T}\right)^2\right),$$
$$C_{200}=\frac{1}{32}\left(\frac{J}{T}\right)^2+o\left(\left(\frac{J}{T}\right)^2\right), \quad \text{(B.16)}$$

cf. Eq. (4.16).

References

1. C. Lhuillier and G. Misguich, in *High Magnetic Fields: Applications in Condensed Matter Physics and Spectroscopy*, Lecture Notes in Physics Vol. 595, edited by C. Berthier, L. P. Lévy, and G. Martinez (Springer, Berlin, 2002), pp. 161-190; G. Misguich and C. Lhuillier, in *Frustrated Spin Systems*, edited by H. T. Diep (World Scientific, Singapore, 2005), pp. 229-306; J. Richter, J. Schulenburg, and A. Honecker, in *Quantum Magnetism*, Lecture Notes in Physics Vol. 645, edited by U. Schollwöck, J. Richter, D. J. J. Farnell, and R. F. Bishop (Springer, Berlin, 2004), pp. 85-153.
2. Д. Н. Зубарев, *Неравновесная статистическая термодинамика* (Наука, Москва, 1971) (in Russian).
3. С. В. Тябликов, *Методы квантовой теории магнетизма* (Наука, Москва, 1975) (in Russian).
4. Д. Н. Зубарев и Ю. А. Церковников, Труды Математического института АН СССР **175**, 134 (1986) (in Russian).
5. N. M. Plakida, Theoretical and Mathematical Physics **168**, 1303 (2011).
6. Yu. G. Rudoy, Theoretical and Mathematical Physics **168**, 1318 (2011).
7. І. В. Стасюк, *Функції Гріна у квантовій статистиці твердих тіл* (ЛНУ імені Івана Франка, Львів, 2013) (in Ukrainian).
8. J. Kondo and K. Yamaji, Prog. Theor. Phys. **47**, 807 (1972).
9. S. Winterfeldt and D. Ihle, Phys. Rev. B **56**, 5535 (1997).
10. D. Ihle, C. Schindelin, A. Weiße, and H. Fehske, Phys. Rev. B **60**, 9240 (1999); D. Ihle, C. Schindelin, and H. Fehske, Phys. Rev. B **64**, 054419 (2001).
11. L. Siurakshina, D. Ihle, and R. Hayn, Phys. Rev. B **61**, 14601 (2000).
12. I. Juhász Junger, D. Ihle, and J. Richter, Phys. Rev. B **80**, 064425 (2009).
13. M. Härtel, J. Richter, O. Götze, D. Ihle, and S.-L. Drechsler, Phys. Rev. B **87**, 054412 (2013).
14. Yu. A. Tserkovnikov, Theoretical and Mathematical Physics **154**, 165 (2008).
15. A. W. Sandvik, Phys. Rev. Lett. **80**, 5196 (1998).
16. A. J. F. de Souza and M. L. Lyra, Phys. Rev. B **65**, 100405(R) (2002).
17. M. Troyer, F. Alet, and S. Wessel, Brazilian Journal of Physics **34**, 377 (2004).
18. S. Wessel, Phys. Rev. B **81**, 052405 (2010).

19. A. F. Albuquerque et. al., J. Magn. Magn. Mater. **310**, 1187 (2007); B. Bauer et. al., J. Stat. Mech. P05001 (2011).
20. А. П. Прудников, Ю. А. Брычков и О. И. Маричев, *Интегралы и ряды. Элементарные функции* (Наука, Москва, 1981), с. 584 (in Russian).
21. T. Kawabe and I. Mannari, Prog. Theor. Phys. **50**, 1474 (1973).
22. H. Shimahara and S. Takada, J. Phys. Soc. Jpn. **60**, 2394 (1991).
23. D. Schmalfuß, R. Darradi, J. Richter, J. Schulenburg, and D. Ihle, Phys. Rev. Lett. **97**, 157201 (2006).
24. A. A. Vladimirov, D. Ihle, and N. M. Plakida, Theoretical and Mathematical Physics **177**, 1540 (2013).
25. A. F. Barabanov, V. M. Beresovsky, and E. Žąsinas, Phys. Rev. B **52**, 10177 (1995).
26. A. V. Miheyenkov, A. V. Shvartsberg, and A. F. Barabanov, JETP Letters **98**, 156 (2013).
27. R. Schmidt, J. Schulenburg, J. Richter, and D. D. Betts, Phys. Rev. B **66**, 224406 (2002); K. Majumdar and T. Datta, J. Phys.: Condens. Matter **21**, 406004 (2009); K. Majumdar, J. Phys.: Condens. Matter **23**, 046001 (2011); W. Nunes, J. R. Viana, and J. R. de Sousa, J. Stat. Mech. P05016 (2011).
28. O. D. R. Salmon, N. Crokidakis, M. A. Neto, I. T. Padilha, J. R. Viana, and J. R. de Sousa, arXiv:1208.5469.
29. G. A. Baker, Jr., H. E. Gilbert, J. Eve, and G. S. Rushbrooke, Phys. Rev. **164**, 800 (1967).
30. J. Oitmaa and E. Bornilla, Phys. Rev. B **53**, 14228 (1996).
31. H.-J. Schmidt, A. Lohmann, and J. Richter, Phys. Rev. B **84**, 104443 (2011); A. Lohmann, H.-J. Schmidt, and J. Richter, Phys. Rev. B **89**, 014415 (2014).
32. C. M. Soukoulis, S. Datta, and Y. H. Lee, Phys. Rev. B **44**, 446 (1991).
33. A. Zander, *Diplomarbeit: Anwendung von Greenschen Funktionen auf Quantenspinsysteme* (Magdeburg, 2013) (in German).
34. P. Müller, *Diplomarbeit: Methode der Greenschen Funktionen zur Analyse frustrierter Quantenspinsysteme* (Magdeburg, 2014) (in German).

CONDENSED MATTER PHYSICS

The journal **Condensed Matter Physics** is founded in 1993 and published by Institute for Condensed Matter Physics of the National Academy of Sciences of Ukraine.

AIMS AND SCOPE: The journal **Condensed Matter Physics** contains research and review articles in the field of statistical mechanics and condensed matter theory. The main attention is paid to physics of solid, liquid and amorphous systems, phase equilibria and phase transitions, thermal, structural, electric, magnetic and optical properties of condensed matter. Condensed Matter Physics is published quarterly.

ABSTRACTED/INDEXED IN: Chemical Abstract Service, Current Contents/Physical, Chemical&Earth Sciences; ISI Science Citation Index-Expanded, ISI Alerting Services; INSPEC; "Referatyvnyj Zhurnal"; "Dzherelo".

CONTACT INFORMATION:
Institute for Condensed Matter Physics
of the National Academy of Sciences of Ukraine
1 Svientsitskii Str., 79011 Lviv, Ukraine
Tel: +38(032)2761978; Fax: +38(032)2761158
E-mail: cmp@icmp.lviv.ua http://www.icmp.lviv.ua